Stockholm University

Master Thesis

Degree Project in
Geochemistry 60 hp

A test of the use of endospores of thermophilic sulfate-reducing bacteria as oceanographic tracers or bioindicators

Emelie Ståhl

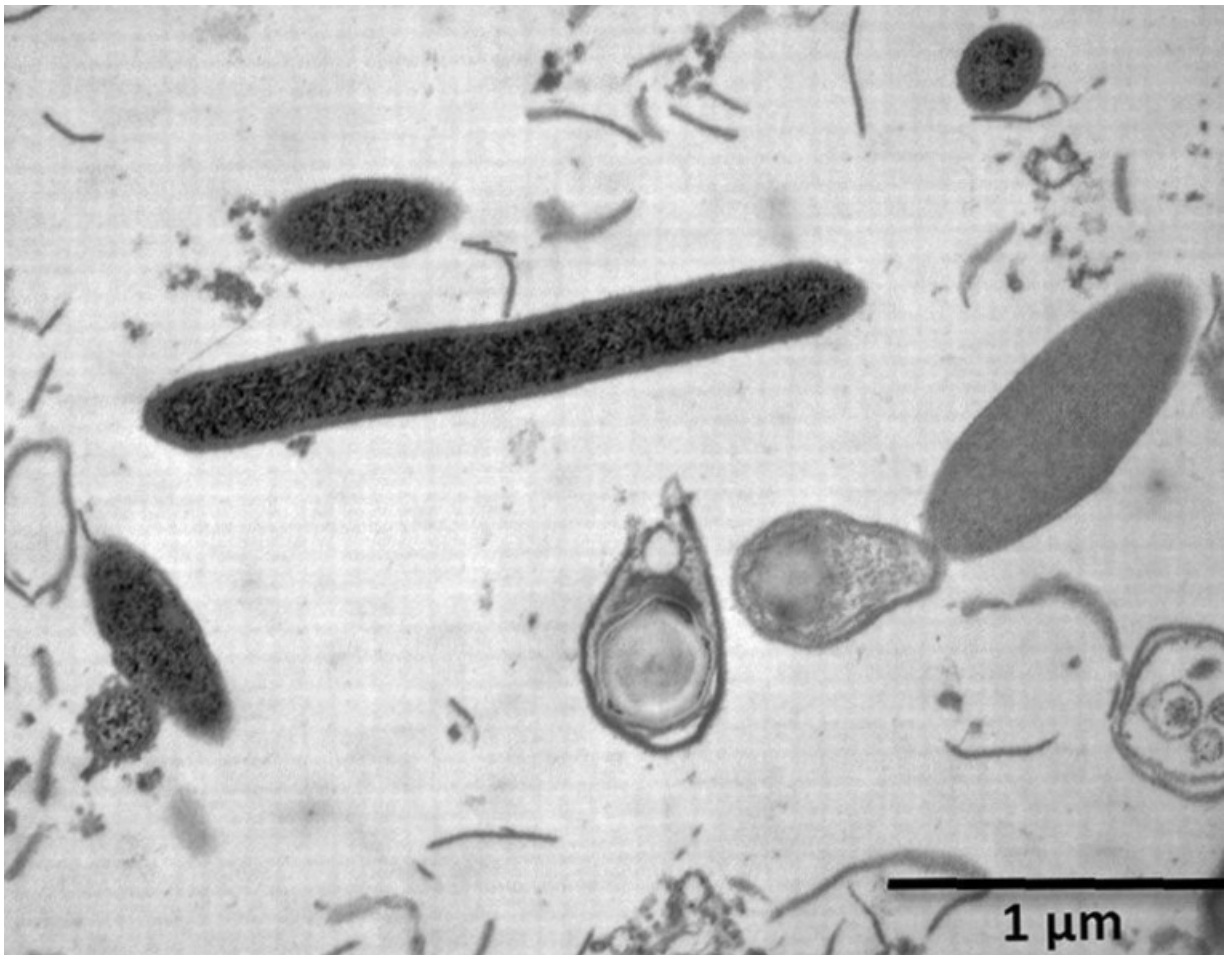

Stockholm 2021

Department of Geological Sciences
Stockholm University
SE-106 91 Stockholm

A test of the use of endospores of thermophilic sulfate-reducing bacteria as oceanographic tracers or bioindicators

Front page: A TEM showing small cells of *Desulfotomaculum Putei* during maintenance metabolism, a few spores, and fragments of cell walls and membranes from cell lysis. From Davidson et al. (2009).

Abstract

The unexpected presence of endospores of thermophilic, sulfate-reducing bacteria have been found in the cold marine seabed all around the world. Since endospores show no metabolic activity at cold in situ temperatures, their presence at such locations indicates that they were passively dispersed by ocean currents from a warm source habitat where they were last active until they settled out of the water column at the site of deposition. Furthermore, their resilient structure can endure harsh conditions and withstand the test of time, thereby leaving a long-term dispersal history in the sedimentary record as they accumulate in the sediment during burial. These properties render endospores a great potential to be used as tracer organisms. This project explores the potential of endospores to be used as oceanographic tracers and bioindicators for hydrocarbon seeps. Temperature gradient experiments using Baltic Sea sediment mixed with artificial seawater media of different salt concentrations were tested as a mean to differentiate between marine versus terrestrial source environments, and radiotracer experiments with Siberian shelf sediments were used to enumerate the number of endospores associated with active seep sites. A lot of focus was also put into optimizing the cultivation method and developing a suitable cultivation medium. The results show that sulfate-reducing bacteria have a metabolic flexibility for growth under various salt concentrations, thus hampering the choice of media as a mean to differentiate between sources. However, a positive correlation was made between a possible thermogenic methane seep and the number of endospores in sediment from the same location, indicating a promising use of endospores as bioindicators for hydrocarbon seeps. If this correlation can be confirmed, this would provide a useful tool to help constrain the origin of methane in Siberian shelf sediments, which is important in our understanding concerning how methane releases will develop in a warming climate. The identity of the detected endospores could not be deduced within the scope of this project however, without which their true origin remains highly speculative.

Table of contents

1. Introduction

Metabolically dormant endospores of thermophilic sulfate reducing bacteria (tSRB) in the cold marine seabed have been found in several locations around the world following their first discovery in sediments from Aarhus Bay, Denmark (Isaksen et al., 1994). Since cold environments cannot support growth of these conspicuous bacteria, their presence in such areas implies that they must have been transported from a warm source habitat where they were last active to their present location (Isaksen et al., 1994; Hubert et al., 2009; de Rezende et al., 2013; Müller et al., 2014). Their dormant state also implies that they are not sensitive to selection factors leading to spatial differentiation or extinction (de Rezende et al., 2013). Their distribution in the marine seabed is therefore mainly due to passive transport, highly controlled by source location and dispersal vectors such as ocean currents (Hubert et al., 2009; de Rezende et al., 2013; Müller et al., 2014). It has been shown that endospores can remain dormant but viable for thousands (de Rezende et al., 2013), maybe up to millions of years (Cano&Borucki, 1995), thereby leaving a long-term dispersal history in the sedimentary record. These properties render endospores a great potential to be used in biogeography studies (Bell et al., 2018).

Apart from natural source habitats, endospores from tSRB can also have an anthropogenic origin (Isaksen et al., 1994; de Rezende et al., 2013). In sediments from River Tyne, northeast England, endospores from anthropogenic sources were thought to originate from historic mining activities as well as of various contemporary industrial discharges. Wastewaters from North Sea oil fields were also identified as a possible anthropogenic source (Bell et al., 2018). Similar to the Tyne sediments, some endospores found in Aarhus Bay were thought to originate from wastewater treatment plants, coal-fired power stations, as well as distant oil fields (Isaksen et al., 1994; de Rezende et al., 2013). In addition to uses as model organisms in biogeography studies, endospores and endospore-forming bacteria have thus been proposed to have a potential as bioindicators to screen for the extent of anthropogenic pollution (Bell et al., 2018). It has also been suggested that certain microorganisms may be used as bioindicators for thermogenic hydrocarbons, and hence have a potential to be used in oil- and gas- prospecting (Hubert&Judd, 2010). However, the usage of endospores as tracer or indicator organisms is dependent on our ability to differentiate between possible source habitats, which in turn means that endospores from different origins must be measurably distinct (Hubert&Judd, 2010; Bell et al., 2018).

This project is an experimental pilot study investigating the presence of endospores of tSRB in sediments from two different locations with different water sources and presumably very different source habitats. The first location to be investigated is the Western Gotland Basin (WGB) in the Baltic Sea (Fig. 1), which is one of the world´s largest brackish-water bodies, linking its inland tributaries with the North Sea (Leppäranta&Myrberg, 2009). In resemblance to the Tyne estuary, the Baltic is highly contaminated since it is surrounded by highly industrialized countries, which is further enhanced by a limited water exchange with the North Sea (Larsson et al., 1985). The second location to be investigated is the East Siberian Arctic Shelf (ESAS) (Fig. 2). ESAS is characterized by its large and shallow shelf system, harbouring enormous amounts of carbon stored as gas hydrates, subsea permafrost, gas pockets, and deep reservoirs of thermogenic gas (Cramer&Franke, 2005; Sapart et al., 2017; Steinbach et al., 2021; Baranov et al., 2020). In the wake of anthropogenic warming, an increasing concern has risen about how much methane these different subsea sources hold, and how much they could contribute to amplify future global warming (Steinbach et al., 2021).

Figure 1: Map of sample location BBL2 in the WGB.

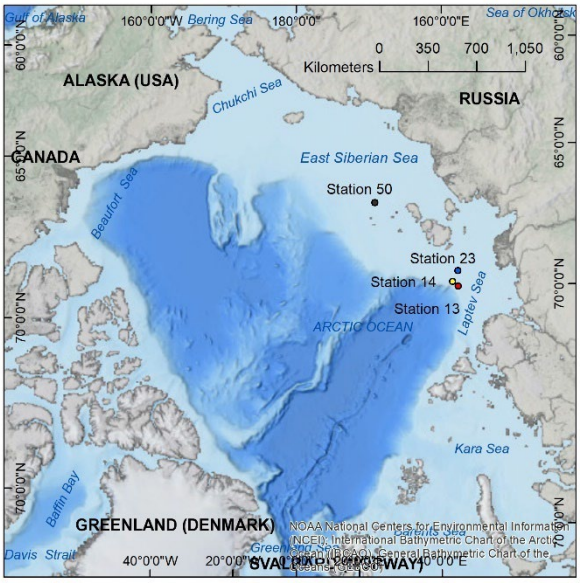

Figure 2: Location of station 13, 14, 23, and 50 in the ESAS.

2. Background

2.1. Endospores in the cold marine seabed

Mai Isaksen with colleagues were probably among the first who investigated anaerobic thermophilic spore-forming bacteria. During a temperature gradient experiment with sediment from Aarhus Bay, they made a surprising discovery that bacteria grew by sulfate-reduction in samples heated to 60℃, indicating a presence of endospores from thermophilic bacteria despite in situ temperatures never exceeding 15℃ (Isaksen et al., 1994). A few years later, Barnes and colleagues detected endospores in permanently cold sediments from Cascadia Margin, Northeast Pacific, presumed to belong to the endospore forming sulfate-reducing genus *Desulfotomaculum* (Barnes et al., 1998). Endospores from tSRBs were further investigated during the next-coming years, including several studies involving quantitative estimates and phylogenetic relationships. Hubert et al. (2009) performed phylogenetic analysis of spore-forming thermophilic bacteria in Svalbard sediments, and estimated a constant delivery of endospores of tSRB at a rate exceeding 10^8 spores per m^2/year. de Rezende et al. (2013) investigated Aarhus Bay sediments and could reveal twenty-three species-level phylotypes of *Desulfotomaculum* spp, of which three were highly similar to the tSRB that were previously detected in the Svalbard sediments (Hubert et al., 2009; 2010; de Rezende et al., 2013). Since it is roughly 3000 km between these two locations, this finding indicated a long-distance dispersal of tSRB originating from a source common to both locations (de Rezende et al., 2013). A recent investigation of global total endospore abundance in the marine subsurface, estimated a population of up to 1.9 x 10^{29} endospores in the uppermost kilometre of sediment, thus surpassing the estimated vegetative cell population (i.e. the population of metabolically active and replicating bacteria) of 8.5 x 10^{28} by almost one order of magnitude (Wörmer et al., 2019). Clearly, the distribution of endospores is widespread, and their abundance in the marine seabed is numerous.

2.1.1. Spore formation, germination and outgrowth

The process of endospore formation is an ability acquired by some members of the phyla *Firmicutes,* notably within the classes *Bacilli* and *Clostridia.* Studies on the various processes involved in spore formation, germination, and outgrowth have mainly been performed on the aerobic model

bacterium *Bacillus subtilis* and to a lesser extent on some pathogenic species within the order *Clostridiales,* such as *Clostridium perfringens* (Paredes-Sabja et al., 2011; Christie&Setlow, 2020). Studies on different *Desulfotomacula* are particularly scarce (Vecchia et al., 2014) and the following description is therefore primarily based on *B. subtilis*, but it must be highlighted that the exact processes involved in sporulation, germination, and outgrowth differs both among classes as well as between species (Paredes-Sabja et al., 2011; Vecchia et al., 2014; Christie&Setlow, 2020).

The process of endospore formation, or sporulation, where an active vegetative cell becomes a dormant endospore is characterized by a considerable morphological and biochemical change occurring in several stages (summarized in Fig. 3). Sporulation begins with the formation of a small compartment, referred to as the forespore, inside the "mother cell". Initially the forespore and the mother cell reside side by side, separated by a flat polar septum and held together by the external cell wall. The forespore is then engulfed by the mother cell, producing a double membrane-bound forespore that resides inside the mother cell´s cytosol (Setlow, 2007; Tan&Ramamurthi, 2014). Further maturation inside the mother cell includes the formation of a thick peptidoglycan cortex sandwiched between the outer and inner membrane. The cortex formation is associated with a decrease in volume and water content as well as a decrease in pH. The mother cell synthesizes large amounts of Dipicolinic acid (DPA) which is incorporated into the forespore at further expense of the water content in the maturating spore. In the last stages of spore formation, an outer complex proteinaceous coat layer is formed by spore-specific proteins produced by the mother cell (Setlow, 2007; Vecchia et al., 2014). Some species, including *Desulfotomaculum* spp. (Vecchia et al., 2014), also form an outermost balloon-like layer called exosporium. The partly dehydrated, metabolically dormant endospore is then released into the environment as the mother cell lyse (Setlow, 2007; Vecchia et al., 2014).

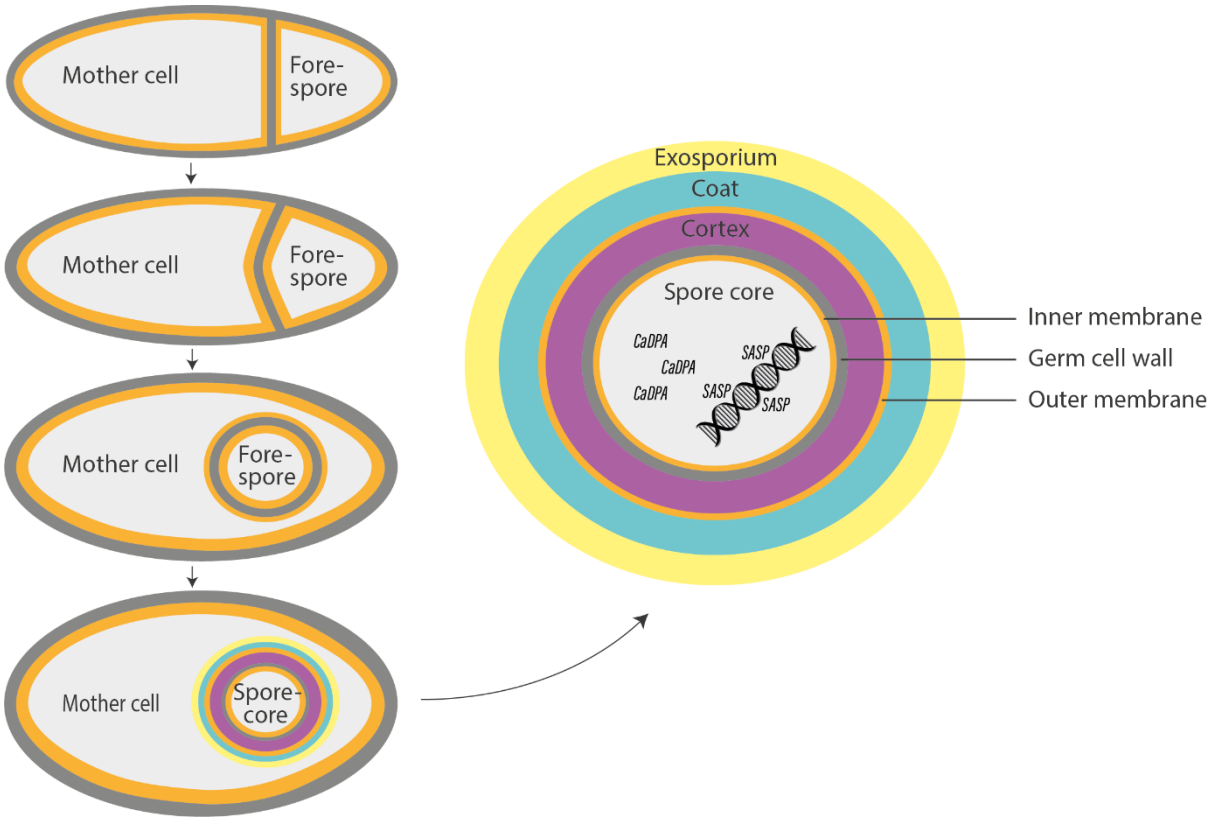

Figure 3: Illustration of the sporulation process and the endospore structure. Adapted from Setlow et al., 2017.

Since the spore needs to survive without nutrients for an unknown amount of time, potentially thousands or millions of years (de Rezende et al., 2013; Cano&Borucki, 1995), the spore must remain in a metabolically inactive state (Foster&Johnstone, 1990; Setlow, 2006). Furthermore, since the endospore cannot predict in which environment it will end up, it must also be able to resist various harsh conditions. Indeed, the spore is one of nature´s most resilient biological structures and, apart from nutrient deprivation, can withstand exposure to toxic chemicals, γ- and UV- radiation, desiccation, and extreme heat (Foster&Johnstone, 1990; Setlow, 2006; 2007), thus allowing for protection and preservation of genetic material until conditions become favourable again. There are many factors contributing to the resilience of the endospore, the most important being i) the protective outer core layer, important for protection against harmful chemicals ii) the spore cortex peptidoglycan layer, which establishes and maintains the core´s low water content (Nicholson et al., 2000; 2002; Setlow, 2007; Christie&Setlow, 2020), and is thought to be responsible for the lack of metabolism and enzymatic activity due to protein immobility induced by the low water content (Cowan et al., 2003) iii) the condensed inner membrane in which lipids have a very low mobility, creating a very impermeable layer which protects the spore from DNA-damaging chemicals iv) high levels (ca 25% of core dry weight) of DPA complexed with Ca^{2+} and other divalent cations in the spore core, important for DNA protection against heat and desiccation among other things, and v) saturation of the spore DNA with a group of small, acid-soluble spore proteins (SASP), which together with Ca-DPA acts to protect the DNA (Nicholson et al., 2000; 2002; Setlow, 2007; Christie&Setlow, 2020). The ambient temperature at the time sporulation occurred also influences the endospores resistance against heat, which therefore can vary even between individual spores within the same species (Nicholson et al., 2000).

However, in order to be a successful survival strategy, the endospore must monitor their environment to be able to reactivate and grow once environmental conditions become favourable again (Foster&Johnstone, 1990). The process of reactivation from a dormant endospore to a vegetative cell starts with germination, defined as the period beginning with the addition of a germinant (molecules that trigger spore germination) and ending approximately at the time metabolism initiates (Paidhungat&Setlow, 2002). Most germinants are nutrients and species-specific (Paredes-Sabja et al., 2011). Somewhat surprisingly, since ATP production is not needed for initiation of germination, the nutrient germinants are merely acting as signalling molecules and do not have any role in actual metabolism (Donnelly&Busta, 1982; Paidhungat&Setlow, 2002; Paredes-Sabja et al., 2011). The germinant binds to specific ligand binding sites on special germinant receptors (GRs), which respond by initiating a cascade of biochemical events. However, it is not fully understood how germinants bind to GRs and exactly how they influence their function (Foster&Johnstone, 1990; Paredes-Sabja et al., 2011; Zhang et al., 2010). DPA and its chelated divalent cations are released early in the germination process and is subsequently replaced by water. The final stage of spore germination includes the hydrolysis of the spore peptidoglycan cortex (Paredes-Sabja et al., 2011; Christie&Setlow, 2020) resulting in an approximate 2-fold expansion of the spore core and a remodelling of the germinating cell wall and inner membrane. The spore core water content increases in the transformation of the dormant endospore from around 45% to a final 80% in the vegetative cell (Christie&Setlow, 2020). The large increase in volume associated with this metamorphosis ultimately leads to the escape from the surrounding spore coat structure. This final stage is referred to as outgrowth, which is also characterized by initiation of metabolism. However, germination and outgrowth are overlapping events, and there is not a clear distinction between the two (Paidhungat&Setlow, 2002). The difference in morphology between an endospore and a vegetative cell can be seen in Figure 4.

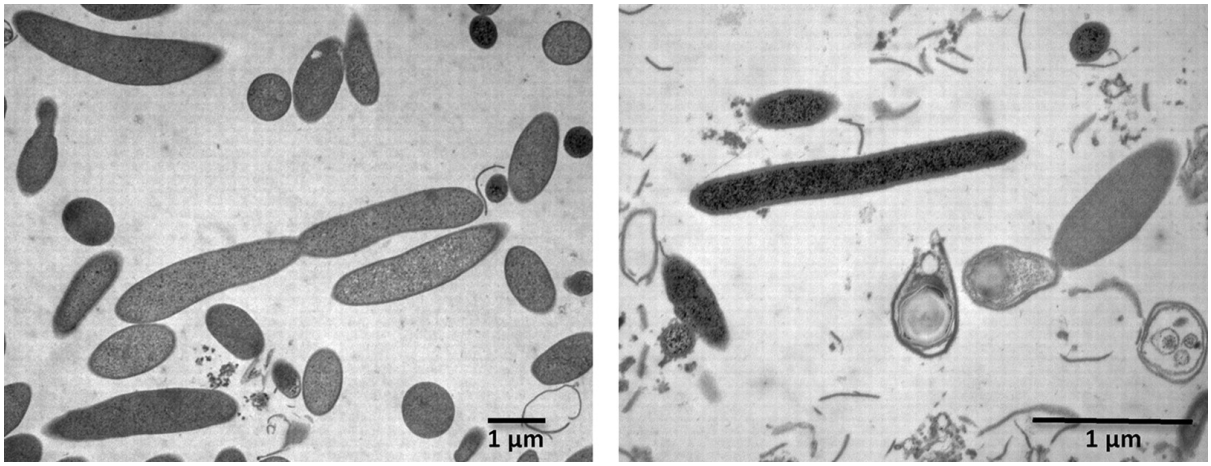

Figure 4: The left figure shows a transmission electron micrograph (TEM) of large vegetative cells of Desulfotomaculum putei. *The large cell in the centre is dividing. The figure to the right shows smaller cells during maintenance metabolism, a few spores, and fragments of cell walls and membranes from cell lysis. From Davidson et al. (2009).*

2.2. Sulfate-reducing bacteria

2.2.1. Classification

The taxonomy of SRB and other prokaryotes has traditionally been based on physical properties such as cell shape, motility, optimal temperature, type of electron donor, and complete versus incomplete oxidation of acetate (Castro et al., 2000). Modern taxonomy is now primarily based on gene sequencies, commonly using a marker gene that encodes for the 16S ribosomal RNA (rRNA) (Stackebrandt et al., 1997; Castro et al., 2000; Muyzer et al., 2008). However, reclassifications due to inconsistencies between traditional and modern classification frequently occur, which may lead to a deviation between a since long accepted name and its taxonomic concept. To further complicate things, it does not even exist an official taxonomy for prokaryotes (Garrity, 2016).To disentangle the problems associated with the taxonomic jungle of microorganisms is far beyond the scope of this project, but they are worth highlighting since both taxonomy, species, and their assigned names are subject to change, which might render inconsistencies and errors in the literature and thereby a likely source of confusion (Garrity, 2016). Adopting the taxonomy from NCBI, all known endospore-forming thermophilic sulfate-reducing bacteria are members of the family *Peptococcaceae*, order *Clostridiales*, class *Clostridia* and phylum *Firmicutes* (Stackebrandt et al., 1997).

The dominating genus within the endospore-forming SRB is *Desulfotomaculum,* which was created 1965 by Campbell and Postgate to describe and separate sporulating from non-sporulating SRB. The name *Desulfotomaculum* was derived from the prefix *''Desulfo''* to indicate the reduction of sulfur compounds, and the suffix *''-tomaculum'',* the latin word for sausage in resemblance to the typical cell shape of this genus (Campbell&Postgate, 1965), which is typically straight or curved and commonly between 2.5 to 15 µm in length and 0.3 to 2.5 µm wide (Fig. 4). Endospore-containing bacteria usually swells due to the round or oval spore, which often has a central or terminal position (Aüllo et al., 2013). Since 1965 the group of endospore-forming SRB has been complemented by the genera *Desulfosporosinus* (Stackebrandt et al., 1997; Vatsurina et al., 2008), *Desulfosporomusa* (Sass et al., 2004), *Desulfovirgula* (Kaksonen et al., 2007a), *Desulfurispora* (Kaksonen et al., 2007b), and the enigmatic genus *Candidatus Desulforudis* (Chivian et al., 2008; Karnachuk et al., 2019).

2.2.4. Biochemistry of sulfate-reduction

SRB and other sulfate-reducing prokaryotes is a diverse group of organisms that has the ability to respire sulfate (Rabus et al., 2015). During the respiratory process, called dissimilatory sulfate-

reduction (DSR), ATP is synthesized by coupling the oxidation of an organic substrate (the primary electron donor) to the reduction of sulfate (the terminal electron acceptor), ending with the formation and subsequent excretion of hydrogen sulfide (Castro et al., 2000; Rabus et al., 2015). Most of this sulfide is reoxidized back to sulfate by oxidizing sulfur bacteria, thus forming the base of the biological sulfur cycle (Rabus et al., 2015). The metabolic fate of a particular substrate can involve incomplete oxidation with a subsequent release of an intermediate break-down product (commonly acetate), or complete oxidation to CO_2 (Hansen, 1994; Detmers et al., 2001). Examples of some sulfate-reducing reactions with commonly used organic substrates can be seen in Table 1 below.

Table 1: Sulfate-reducing reactions with some common organic substrates, some of which are characteristically only partially oxidized (adapted from Detmers et al., 2001).

Electron donor (type of oxidation)	**Stoichiometry**	ΔG^0 $[kJ\ mol^{-1}(SO_4)^{2-}]$
Lactate (incomplete)	$2\ CH_3CHOHCOO^- + SO_4^{2-} \rightarrow 2\ CH_3COO^- + 2\ HCO_3^- + HS^- + H^+$	*-160.1*
Formate	$4\ HCOO^- + SO_4^{2-} + H^+ \rightarrow 4\ HCO_3^- + HS^-$	*-146.9*
Propionate (incomplete)	$4\ CH_3CH_2COO^- + 3\ SO_4^{2-} \rightarrow 4\ CH_3COO^- + 4\ HCO_3^- + 3\ HS^- + H^+$	*-50.2*
Butyrate (complete)	$CH_3CH_2CH_2COO^- + 2.5\ SO_4^{2-} \rightarrow 4\ HCO_3^- + 2.5\ HS^- + 0.5\ H^+$	*-49.2*
Acetate (complete)	$CH_3COO^- + SO_4^{2-} \rightarrow 2\ HCO_3^- + HS^-$	*-47.6*

The sulfate ion cannot readily diffuse across the cell membrane, and thus needs to be transported into the cell by specialized membrane transport proteins. Since the sulfate concentration in the environment can vary from high levels of around 28 mM in seawater to less than a few μM in freshwater, SRBs have developed different approaches to efficiently transport sulfate into the cell at different sulfate concentrations. In sulfate-limited environments, a high accumulating active transport of sulfate occurs in symport with three cations (either H^+ or Na^+). Since the excretion of sulfide leads to a removal of two protons, either as H_2S or as HS^- in symport with H^+, it leads to a net charge across the membrane at the cost of about one-third ATP per sulfate. However, in environments not limited in sulfate, a low-accumulating transport of sulfate operates with an electroneutral symport with two cations, which is energetically more favourable (Rabus et al., 2015; Marietou et al, 2018). After entering the cell, the stable sulfate anion must be activated in an ATP-consuming process before use. The reduction of sulfate is then coupled to an electron transport chain driven by the net difference in reduction potentials between the primary electron donor and the terminal electron acceptor (i.e. sulfate), which is used to generate a transmembrane proton-gradient and the synthesis of ATP. The pathways involving the 8-electron reduction of sulfate to sulfide is not entirely understood, but likely proceeds via several reactions with each reaction step producing sulfur species with intermediate oxidation states (Rabus et al., 2015).

2.3. Habitats of tSRB

Most studies targeting endospores from tSRB in the cold marine seabed have found that the abundance of spores is surprisingly large, and the microbial endospore-forming community is diverse. This has led to the common interpretation that multiple sources from different source environments may supply endospores to the cold marine seabed. Furthermore, the warm and anaerobic source habitat must have a sufficient magnitude to support the observed population sizes (Hubert et al., 2009; de Rezende et al., 2013).

2.3.1. Marine habitats

A limited number of warm source habitats in the marine realm have been identified that can support the magnitude necessary to explain the numbers of endospores in the cold marine seabed (Hubert et al., 2009; de Rezende et al., 2013). Oil and gas reservoirs located some 2 to 4 km below the seafloor can have a typical temperature range between 50 to 120℃ (given a normal geothermal gradient between 25 to 30℃ per km, Lowell et al., 2014), thus having a potential as a likely source habitat for tSRB (Hubert et al., 2009; de Rezende et al., 2013). The upward emigration of hydrocarbon gas may transport endospores and other microorganisms from these deep reservoirs. After subsequent expulsion at seep sites, ‘‘hitch-hiking’’ endospores may be carried away by ocean currents and deposited at some distance away from the seep (Hubert&Judd, 2010). However, most microbial studies concerning the deep subsurface, which have increased in numbers since the early 1980´s, are associated with industrial activities (i.e. oil production) (Magot et al., 2000; Frank et al., 2016). From these studies it is apparent that several endospore-forming microorganisms, including various *Desulfotomaculum* spp., are present in different oil field environments around the world (Rosnes et al., 1991; Magot et al., 2000; Frank et al., 2016). In Chinese oilfields with depths between 1300 and 1490 m and temperatures between 58 and 63℃, as much as 70 – 80% of the investigated phylogenetic groups consisted of different *Desulfotomaculum* spp. (Guan et al., 2013). However, there is some debate concerning if endospores from SRBs in oil fields are occurring natively in the environment or if they are brought into the reservoir by seawater injection associated with oil production operations, thus their true origin remains speculative (Rosnes et al., 1991; Magot et al., 2000; Frank et al., 2016).

Endospores from tSRB may also originate from warm deep sediments and ocean crust brought to the surface via hydrothermal circulation associated with spreading mid-ocean ridges (Hubert et al., 2009; de Rezende et al., 2013). In an extensive study by Müller et al. (2014), it was found that sediment associated with hydrothermal circulation in the Guaymas Basin hosted large numbers of endospores, including species of different *Desulfotomaculum* spp. (Müller et al., 2014). *Desulfotomaculum* species have also been found in microbial mats from a hydrothermal vent located in the Lost City active hydrothermal field associated with the Mid-Atlantic Ridge (Gerasimchuk et al., 2010), and in sediments around a hydrothermal vent situated in the Tofua Arc in the Tonga Trench (Cha et al., 2013).

2.3.2. Terrestrial habitats

Endospores from various terrestrial sources are commonly found in marine sediments, some of which are thought to originate from industrial activities such as wastewater treatment plants and coal fired power stations (Isaksen et al., 1994; Hubert et al., 2009; Bell et al., 2018). A few examples of industry-related sources are bioreactors treating paper mill wastewater (Parshina et al., 2005), cooling towers within petroleum refineries (Anandkumar et al., 2009), and fluidized-bed reactors treating acidic metal-containing wastewater. *Desulfotomaculum* spp. have also been isolated in locations so diverse as hot solfataric fields in the volcanic Krafla area, north-east Iceland (Goorissen et al., 2003) to rice paddy soils in Vercelli, northern Italy (Stubner&Meuser, 2000). Findings from the deeper terrestrial realm include endospores from tSRB isolated from an underground mine located 250 m below ground in Japan (Kaksonen et al., 2007a), as well as in samples collected from a gas storage aquifer > 800 m below ground in France (Basso et al., 2009).

2.4. Biogeography

In order to better understand how endospores can be used as an oceanographic tracer, it is important to understand the concept biogeography (the study of distribution of organisms across the Earth, and the processes that generate and maintain biodiversity). Four fundamental processes

that have a large influence on microbial biodiversity are selection, genetic drift, mutation, and dispersal. The process of environmental selectivity for individuals that are better adapted to the local conditions generally acts to differentiate the microbial composition between locations, which strengthens the so-called distance-decay relationship (Hanson et al., 2012). An example of such an environmental factor is salinity, which have a strong influence on the microbial taxa. Therefore, in a setting like a coastal estuary, two locations situated near the ocean will likely have a more similar microbial composition adapted to saline conditions compared to a location further inland (Bell et al., 2018). Genetic drift also acts to strengthen the distance-decay relationship. Random events such as reproduction, deaths, and migration will lead to a differentiation in the microbial composition irrespective of the surrounding environment. Genetic mutations also increase the local genetic diversity. On the contrary, dispersal acts to counteract the differentiation in microbial composition between different locations (Hanson et al., 2012). An organism can disperse by active or passive transport. Active transport of microorganisms can take place by active propulsion, such as propelling itself with its flagella. As can be imagined, this way of dispersing does not take the organism very far. Microorganisms can also be dispersed by passive transport. In contrast to active dispersal, passive dispersal can carry a microorganism thousands of kilometres, for example by winds or ocean currents (Martiny et al., 2006). With limited dispersal, the composition in one location will be more similar to nearby locations than to those further away. However, when dispersal rates increase, the local composition will increasingly reflect that of the newly established colonizers (Hanson et al., 2012), rather than the result of environmental selection, genetic drift, and mutations. If the dispersal is high enough, the compositional differentiation due to selection, drift, and mutation will be entirely cancelled out (Hanson et al., 2012).

Since endospores are metabolically inactive, it implies that they are not sensitive to the above-mentioned selection factors (de Rezende et al., 2013). Furthermore, since cold environments cannot support their growth, their presence in such areas implies that they must have been transported from a warm source habitat to their present location (Isaksen et al., 1994; Hubert et al., 2009; de Rezende et al., 2013; Müller et al., 2014). Their distribution in the marine seabed is therefore due to passive transport, highly controlled by source location and dispersal vectors (Hubert et al., 2009; de Rezende et al., 2013; Müller et al., 2014). These properties render endospores a great potential to be used as an oceanographic tracer and/or bioindicator.

2.5. Methods for cultivating and quantifying the activity of endospore forming tSRB

2.5.1. Growth media, heat activation, and pasteurization

Due to the resilient nature of the endospore, there is currently a lack of reliable culture-independent methods due to the difficulty with exctracting their DNA (Wunderlin et al., 2013). Therefore, culture-dependent methods are commonly deployed to reveal their abundance and identification. Media used for the cultivation of microorgansims must contain substances that support their growth. General requirements for a cultivation media include a source of carbon and nitrogen, buffers to maintain a suitable pH, and growth factors such as trace elements (Pepper&Gerba, 2015). Many different media have been used to culture SRB, and they can be designed to be more or less inclusive of different physiological types of organisms. However, a medium that is well suited for all kinds of SRB does not exist. Moreover, since SRB grow under anoxic, reducing conditions, removing oxygen is essential to facilitate initiation of cell growth and prevention of oxygen-induced cell damage. Removal of oxygen only by physical means (for example by purging with N_2) may not be sufficient, and addition of reductants to the growth medium may be necessary (Widdel&Bak, 1992). A vast variety of organic substrates can serve as both energy- and carbon source for SRB in anoxic

environments. However, they rarely utilize organic macromolecules. Instead, they use typical fermentation and intermediate break-down products, such as certain amino acids, glycerol, and volatile fatty acids (VFAs) such as acetate, lactate, butyrate, and propionate (Hansen, 1994).

Endospore activation treatments, commonly using a sublethal heat-shock, can decrease the lag-time between the addition of a germinant and initiation of germination. Furthermore, it may increase the synchrony of germination of a spore population. The precise effect of heat activation is not fully known (Foster&Johnstone, 1990; Paidhungat&Setlow, 2002), but it is thought to increase the amount of activated and functional GRs per spore (Zhang et al., 2010). Yet it was shown in a study on endospores from *D. nigrificans* that a prolonged heat-treatment could adversely affect germination. Optimal spore germination occurred after a heat-treatment of 15 to 20 minutes in 100℃. However, different temperatures for the heat-treatment were not tested (Donnelly&Busta, 1982) despite early suggestions that different species may require different temperatures for their optimum heat-treatment, potentially due to differences in their thermal resistance (Evans&Curran, 1943). Pre-heating samples also allows for selective enrichment of endospore-forming bacteria, as high temperatures decimate vegetative cells (te Giffel et al., 1995; Widdel, 2006).

2.5.2. Estimating microbial activity

Estimating microbial activity can be used to evaluate the response of a microbial community to variations in different environmental parameters (such as temperature and salinity) (Parkes&Sass, 2009). Since SRBs reduce sulfate to sulfide (as described previously), one way to estimate bacterial growth is to quantify the reduction of sulfate to sulfide as indicated by decreasing concentrations of sulfate in the sample. This has for example been done in recent studies by Bell et al. (2018; 2020). However, the resolution for short term incubation experiments may not be high enough (Bak et al., 1991) especially if high background values of sulfate and slow sulfate-reduction rates (SRRs) are present. As an illustration, if the sulfate concentration in the sediment is 20 μmol cm^{-3}, and the SRR is 20 nmol cm^{-3} per day, even a modest reduction of 1% of the sulfate content would take 10 days (Røy et al., 2014). Under such circumstances, other techniques such as using radiotracers should be considered (Bak et al., 1991).

Measuring SRR using radiotracer techniques is considered more sensitive compared to techniques based on the removal of sulfate (Parkes&Sass, 2009). Without biological interference, the stable nature of the sulfate anion precludes it from isotope exchange between the sulfur found in sulfate, and the sulfur found in reduced sulfur species (Fossing, 1995; Røy et al., 2014). This is one of the reasons why the radiotracer method using radiolabelled sulfate ($^{35}SO_4^{2-}$) works so well, since the ^{35}S added as sulfate will only be found as reduced inorganic sulfur after having undergone bacterial DSR (Røy et al., 2014). The reduced radiolabelled sulfur will either remain in solution as $H_2{}^{35}S$ or $H^{35}S^-$ (depending on pH), or it can form metal mono- or disulfides (commonly $Fe^{35}S$, $Fe^{35}S_2$) or elemental sulfur ($^{35}S_0$) either by chemical reactions or by isotopic exchange. The isotopic exchange between H_2S and S_0 occurs almost instantaneously and is completed within minutes (Fossing, 1995).

The combined pool of reduced sulfur species derived from SRR is referred to as total reduced inorganic sulfur (TRIS) (Røy et al., 2014; Kallmeyer et al., 2004). A distillation procedure can then be performed to separate TRIS from sulfate by converting TRIS back to H_2S, which subsequently can be flushed out of the sediment using a continuous flow of N_2. Again, the stable nature of sulfate prevents it from being reduced to sulfide without biological interference, thus leaving the residual sediment with the remaining $^{35}SO_4^{2-}$ that has not been converted to TRIS by DSR. The radioactivity of the separated TRIS and the total activity of $^{35}SO_4^{2-}$ can then be determined by scintillation counting, and SRR can be calculated using following equation from Kallmeyer et al. (2004):

$$SRR = [SO_4^{2-}] \times P_{SED} \times \frac{a_{TRIS}}{a_{TOT}} \times \frac{1}{t} \times 1.06 \times 1000 \qquad \textit{Eq. 1}$$

Where SRR is the sulfate-reduction rate (nmol cm^{-3} h^{-1}), $[SO_4^{2-}]$ is the sulfate concentration in the supernatant of the incubated sample (mM), P_{sed} is the sediment porosity (ml cm^{-3}), a_{TRIS} is the radioactivity of TRIS (counts per minute, cpm), and a_{TOT} is the total radioactivity (a_{TRIS} + $a_{sulfate}$, in cpm), and t is the incubation time (h). The factor 1.06 is a correction for the expected isotopic fractionation, and the factor 1000 corrects for the change of units from mM to nmol/cm^3 (Kallmeyer et al., 2004). Even if the method is considered sensitive, a complicating factor is that the formed $H_2{}^{35}S$ can re-oxidize back to $^{35}SO_4^{2-}$. Therefore, the incubation time after radiotracer amendment should preferentially be kept as short as possible (Fossing, 1995).

2.5.3. Estimating growth rates

An active bacterial cell grows for some amount of time before it will divide in half. The time before cell division occurs is highly dependent on growth conditions such as temperature, pH, and nutrient availability (Hagen, 2010). If a successful bacterial cultivation has been made, that is, if the growth medium and the environmental conditions satisfy the needs for the bacteria of interest, the increase in bacterial cell numbers can be measured as a function of time to obtain a growth curve (Maier&Pepper, 2015). The first observable phase of the growth curve often includes a lag phase, which is a period where the growth rate is essentially zero (Maier&Pepper, 2015), or not detectable. This phase likely reflects the time for endospore germination and outgrowth (Hubert et al., 2009; de Rezende et al., 2017). However, as discussed above, the time before germination is highly variable both between species as well as between individual cells. The exact reasons for this heterogeneity are not known but heat activation, specific nutrient germinants, and the number of germinant receptors on the endospore are considered important (Zhang et al., 2010). This phase also includes the time it takes for the active cells to acclimate and grow before the division rate increases and the exponential phase initiates (Hagen, 2010; Maier&Pepper, 2015). The exponential phase is the period where bacteria grow at the maximum rate possible given the growth conditions present (Maier&Pepper, 2015). If the growth conditions are kept constant, the time before each cell division is assumed to be nearly constant. In such a scenario, the numbers of cells (*N*) will increase at a rate (*dN/dt*) proportional to *N*:

$$kN = \frac{dN}{dt} \qquad \textit{Eq. 2}$$

Where the parameter *k* describes the specific growth rate. Integrating the equation above gives the exponential function:

$$N(t) = N_0 e^{kt} \qquad \textit{Eq. 3}$$

Where N_0 is the initial number of cells (Hagen, 2010; Maier&Pepper, 2015).

2.6. Physical setting of sample locations

2.6.1. The Baltic Sea

The Baltic Sea is a small and rather shallow, semi-enclosed brackish sea consisting of several sub-basins. A limited water exchange with the North Sea together with a strong positive freshwater budget is responsible for the prevailing brackish state of the Baltic Sea (Meier&Kauker, 2003). It has a mean anticlockwise ocean circulation and is characterized by having a permanent salinity stratification with limited vertical mixing, and as a result, poorly oxygenated bottom waters. Human impact has increased the nutrient load in the Baltic, leading to increased eutrophication resulting in higher oxygen consumption and expanding anoxic bottom areas (Larsson et al., 1985). The water exchange between the sub-basins is largely controlled by the presence of several sills that separate the basins. The Western Gotland Basin (WGB) is the largest of the Baltic´s basins, with a mean depth of 71 m. The relatively deep and anoxic bottom water in the Gotland basin only gets ventilated irregularly (ca every 10th year or so) when inflow of saline water enters from the North Sea. However, the propagation of the inflowing water is strongly restricted due to the complex bathymetry and the entrainment and mixing with the ambient brackwater. The bottom water temperatures range between 2 to 10℃ throughout the year, and the salinity typically varies between 8.7 – 10.3‰ at around 100 m depth (Leppäranta&Myrberg, 2009).

2.6.2. The Laptev Sea and East Siberian Arctic Shelf

More than half of the Arctic Ocean is comprised of shallow shelves, with the ESAS constituting the major part. The shelves of the East Siberian Sea and the Laptev Sea are part of the ESAS, and are characterized by a complex system of rifts and faults. The seafloor is comprised of a thick sedimentary cover, at some places up to 12 km thick (Baranov et al., 2020), and harbours vast amounts of carbon stored as gas hydrates, subsea permafrost, and deep reservoirs of thermogenic gas. Several investigations in the past few decades have revealed that methane seeps are common features in several locations in this area (Cramer&Franke, 2005; Sapart et al., 2017; Steinbach et al., 2021; Baranov et al., 2020).

The Arctic Ocean is relatively isolated from the Atlantic and the Pacific Ocean. This is because of its surrounding landmasses and the presence of shallow sills that restrict movement of deep waters between the Arctic and its adjacent oceans (Hanson et al., 2019). Inflow of deep water is mainly limited to the eastern Fram Strait or over the Barents Sea. The Atlantic deep water flows eastwards in a cyclonic pattern around the basins, closely following the shelf breaks. The upper water originates both from the Pacific and the Atlantic Ocean, and is modified by a substantial input of season-dependent river runoff, sea-ice melt, and brine from sea-ice formation (Anderson et al., 2017). The salinity in the Laptev Sea and ESAS is about 33 to 34‰, and the bottom temperature is close to the freezing point around -1.8℃ (Baranov et al., 2020). The average sedimentation rate in the Laptev Sea has been estimated to an average of ca 0.5 cm per year (Bauch et al., 2001).

2.7. Aims and outline of this thesis

Since successful germination and growth of endospores is the first step before their use as a tracer or bioindicator can be concluded, a lot of effort was put into the development of an appropriate cultivation media. Moreover, some problems associated with the cultivation method were revealed after commencing with the experiments, which necessitated for an additional set of experiments to be designed to find the cause of insufficiency. Improving and optimizing the cultivation method were obviously considered important in order to obtain trustworthy results, but also essential before

commencing with the radiotracer experiment for safety reasons (considering the involvement of radioactive material).

Sediment from the WGB was investigated for the presence of tSRB using both fresh-, brackish-, and saltwater concentrations. It was hypothesized that by using media with different salt concentrations, it would be possible to differentiate between source environments (i.e. marine or terrestrial sources). If a salt-dependent change could be observed in either temperature optima and/or in the accumulated amount of reduced sulfate, this could imply that different microbial communities adapted to different environmental conditions develop depending on choice of media. If so, using cultivation media with different salt-concentrations could provide a mean to differentiate between marine versus terrestrially derived endospores. However, if there is no detectable change this would imply a metabolic flexibility for growth under both fresh-, brackish-, and marine conditions, thus hampering the choice of media as a mean to differentiate between sources. To test the use as potential bioindicator for hydrocarbon seeps, sediment from the Laptev Sea and East Siberian Sea was chosen, since these are recognized areas harbouring several seeps (Cramer&Franke, 2005; Sapart et al., 2017; Steinbach et al., 2021; Baranov et al., 2020). SRR experiments using radiolabelled sulfate were designed in order to enumerate the amount of endospores present in the sediments.

This project has four overarching aims which are to 1) investigate the presence of *endospores in Baltic and Siberian shelf sediments* 2) evaluate the use of *endospores from tSRB as an oceanographic tracer* 3) explore the potential use of *tSRB as bioindicators for hydrocarbon seeps*, and 4) to identify *problems and uncertainties associated with cultivation of endospores* from tSRBs, with the purpose to refine the methods used to activate and grow endospores.

To reach the aims outlined above following hypotheses will be investigated i) endospores from tSRB are present in sediments from the Baltic Sea and the ESAS ii) different salt concentrations and temperature optima can be used to differentiate between source regions, and iii) the abundance of endospores is higher in sediments close to hydrocarbon seep sites than in sediments located further away.

3. Methods

3.1. Locations and sampling

Sediment material from the WGB was retrieved in August 2020 onboard *R/V Electra* from station BBL2 (58°04.3 N, 18°23.6 E) in ~100 m water depth (Fig. 1). Sediment was collected using a multicorer and stored refrigerated in sealed plastic bags for 2 to 4 months before it was used for experiments. The sediment mainly consisted of finely laminated, dark-coloured silty clay.

Sediment from the ESAS was retrieved during the SWERUS-C3 expedition Leg 1 in 2014 onboard the Swedish icebreaker *Oden*. The sediment was sectioned in different depth intervals and stored in sealed plastic bags kept refrigerated in the dark for 7 years until used in following experiments. Four stations were selected: 13 (76°46.65 N, 125°49.48 E), 14 (76°53.60 N, 127°48.31 E), 23 (76°10.48 N, 129°20.14 E), and 50 (75°45.79 N, 150°31.77 E) (Fig. 2). Station 13 (60 m depth) and 14 (50 m depth) are located in the Laptev Sea in an area were acoustic data during the SWERUS expedition indicated rising gas bubbles and blanking of the seafloor suggestive of active seep sites (SWERUS, 2016). Furthermore, Steinbach et al recently presented chemical work from station 13 and 14 (among others), which showed elevated methane concentrations in the water column. Highest concentrations were found close to the seafloor, which was thought to indicate a subseafloor source (Steinbach et al., 2021). Station 23 (54 m depth) and 50 (43 m depth) are located in the Laptev Sea

and the East Siberian Sea, respectively. During the SWERUS expedition, these were chosen as reference stations with no acoustic or chemical signal of a methane anomaly (SWERUS, 2016). The sediment from station 14 and 23 consisted of sandy silt to silty sand, whereas the sediment from station 13 and 50 were mainly comprised of more fine-grained clayey silt.

3.2. Slurry Preparations

Sediment slurries were prepared by mixing sediment with seawater medium in a 1:2 ratio (w:w) using seawater media described according to Widdel&Bak (1992). Salts of two different forms of sulfate were tested ($MgSO_4$ x $7H_2O$ and Na_2SO_4). The total salt-concentration (including the concentration of sulfate) was adjusted between experiments. The media were also complemented with sodium bicarbonate (2.4 mM of $NaHCO_3$) to increase the buffer capacity. The pH of the media was controlled using a Schott 850 pH meter fitted with a Schott pH combination electrode. Sediment slurries were amended with *Spirulina,* since the degradation of these cyanobacterial cells have proven to provide a rapid production of VFAs (Arnosti et al., 2004; Hubert et al., 2010; Graue et al., 2012; Volpi et al., 2017; Müller et al., 2018). Amendments with complementary VFAs (acetate, pyruvate, lactate, formate, propionate, and butyrate) and addition of a reducing agent (1 mM Na_2S, final concentration) were tested to optimize the growth yield. All media and amendments (except the *Spirulina* powder) were autoclaved by saturated steam sterilization at 121℃ for 30 min. Information about the chemicals used for seawater media and amendments can be found in Appendix A. Trace elements and vitamins were assumed to be present in the sediment and hence omitted.

To ensure that the sediment slurries were homogenous and oxygen-free, mixing was done under constant N_2-flow and continuous stirring using a magnetic stirrer for about 25 minutes. For the TGEs, aliquots of approximately 6 ml were subsequently transferred using a N_2-flushed syringe to N_2-flushed exetainers (Labco) sealed with chlorobutyl septa, or cultivation tubes of the Hungate-type (Glasgerätebau Ochs) sealed with rubber stoppers and screw caps. For the SRR experiment, aliquots of 10 ml were transferred to 20 ml serum vials sealed with black butyl rubber stoppers and aluminium crimp seals. After transfer, the aliquots were immediately pasteurized in 80℃ ± 1℃ for 30 (6 ml samples) to 40 (10 ml samples) minutes and placed in a temperature gradient block (TGB) for the TGEs, or in an oven held at a constant temperature of 50℃ ± 1℃ for the SRR experiment. Replicate samples were prepared for each experiment at regular intervals to verify the results and to estimate the overall uncertainty of the method. The reported uncertainty was based on the calculated standard uncertainty multiplied by a coverage factor (k = 2,), providing a level of confidence of approximately 95%. Information about how the uncertainty calculations were carried out can be found in Appendix C.

3.3. Temperature gradient experiments

Four TGEs (referred to as TGE #1, TGE #2, TGE #3, and TGE #4) using surface sediment (0 – 15 cm) from the WGB were conducted in a TGB, which was cooled in one end with a refrigerating circulator and heated electrically at the other to create a temperature gradient. The temperature span was chosen to cover the potential physiological temperature range of the activated endospores. The temperature was recorded continuously using built-in thermistors as well as controlled manually using glass thermometers placed at regular intervals in the TGB. The temperature at each temperature interval in the TGB was stable within ± 0.5℃ during the entire incubation period. The total incubation time for the different TGEs was varied between 96 to 167 h to find the optimal incubation time. Two types of culturing vials were used (exetainers and culturing tubes of the

Hungate-type). Experimental conditions for each TGE are summarized in table 2. Since a problem with leakage was suspected after the first three TGEs, all the samples in TGE #4 were weighed both prior to and after incubation to be able to monitor possible weight loss. Incubations were terminated by transferring 1.0 to 1.5 ml aliquots of the samples to 2.0 ml centrifugation vials pre-treated with 0.5 to 1.0 ml ZnAc (5%) and subsequently centrifugated at ~1300 rcf for 10 minutes. The supernatant was stored in -20℃ until sulfate analysis using ion chromatography (IC).

During TGE #1, one set of samples from the entire temperature-gradient was terminated once per day during the total incubation time of 96 h, whereas samples from TGE #2, #3, and #4 were incubated the entire incubation time. However, a complementary time-series experiment (TSE) held in an oven at a constant temperature of 50℃ was performed in parallel with TGE #2. The temperature inside the oven was monitored using glass thermometers and was stable within ± 1℃ during the incubation period. The samples were prepared together with the rest of the TGE-samples, but later incubated in the oven. Samples in the TSE were terminated one to two times per day during the total incubation time of 168 h (7 days).

3.4. Control experiments

Due to noisy results in TGE-experiments (see section 4.1.), a set of experiments were designed to evaluate the suitability of the culturing vials in experiments at elevated temperatures. The effect of different amendments (i.e. different organic substrates and the addition of a reducing agent) was also tested.

3.4.1. Vial control

An experiment was performed to test if the concentrations of sulfate and sulfide change during incubation without microbiologic interference, suggestive of oxygen contamination and/or vapour leakage. N_2-flushed exetainers and tubes of the Hungate-type were filled with 6 ml freshwater medium (SO_4^{2-} 28 mM). The medium was prepared in the same way as the sediment slurries described above (i.e. flushed with N_2 and reduced with Na_2S to a final concentration of 1.0 mM), pasteurized in 80℃ for 30 minutes and subsequently placed in the TGB with a temperature range between 15 and 75℃. Samples were also placed in an oven held at a constant temperature of 50℃, from which samples were removed every 24 hours for the total incubation period of 120 h. Samples were weighed regularly during the entire 120-hour long incubation period. All samples were terminated by transferring 1.5 ml to a vial prefilled with 0.5 ml ZnAc (5%) and frozen at -20℃ until sulfide and sulfate analysis using spectrophotometry and IC, respectively. The samples were also continuously weighed to monitor potential weight-loss during the incubation.

3.4.2. Medium control

N_2-flushed serum vials with butyl rubber stoppers sealed with aluminium crimp seals were filled with 6 ml sediment slurry using a N_2-flushed 10 ml syringe. Sediment slurries from the Laptev Sea (station 13) were prepared as described previously using brackish media with Na_2SO_4. Slurries were either amended with only *Spirulina* (~2.5 g/L final concentration), *Spirulina* plus a mixture of VFAs (same kinds and concentrations as in TGE #3 and #4), or *Spirulina*, VFAs, and an addition of a reducing agent (Na_2S, 1 mM final concentration).

*Table 2: Summary of experimental conditions from temperature gradient and control experiments. *$MgSO_4$ **Na_2SO_4*

Experiment	Incubation temp. range (℃)	Incubation duration (h)	Culturing vial(s)	Basal media	SO_4^{2-} (mM)	Organic Substrates (final conc.)	Reducing agent (Na_2S final conc.)
TGE #1	4 – 79	96	Exetainer	Brackish water	8*	Spirulina ~1.5 g/L	–
TGE #2	20 – 80	116 – 168	Exetainer	Saltwater	20*	Spirulina ~2.5 g/L Acetate 1.0 mM Pyruvate 1.0 mM	–
TGE #3	15 – 75	120	Hungate tubes	Fresh-brackish-and saltwater	28**	Spirulina ~2.5 g/L Acetate 2.0 mM Propionate 2.0 mM Butyrate 4.0 mM Lactate 4.0 mM Formate 8.0 mM	1.0 mM
TGE #4	15 – 75	120	Exetainer	Brackish water	28**	Spirulina ~2.5 g/L Acetate 2.0 mM Propionate 2.0 mM Butyrate 4.0 mM Lactate 4.0 mM Formate 8.0 mM	1.0 mM
Vial control	15 – 75	120	Exetainer Hungate tubes	Fresh water	28**	–	1.0 mM
Medium control	50	120	Serum vials	Brackish water	28**	Varied (see 3.4.2.)	Varied (see 3.4.2.)

3.5. Sulfate-reduction rates using radiolabeled sulfate

Surface sediment from ESAS station 13 (0 – 5.5 cm), 14 (2 – 6 cm), 23 (0 – 4 cm), and 50 (0 – 5 cm) were used for a SRR time-series experiment. Sediment slurries were prepared as described above, but 20 ml glass vials with black butyl rubber stoppers and aluminium crimp seals were used instead of exetainers/hungate tubes, and 10 ml slurry aliquots were transferred to each vial instead of 6 ml. Following pasteurization, the samples were incubated at 50℃ for a total incubation time of 120 h (table 3). The incubation temperature was chosen since it is in the range of thermophilic growth and to maintain consistency with previous research in Svalbard sediments (Hubert et al., 2009; de Rezende et al., 2013; 2016). Three times per day subsamples were amended with ca 50 kBq $^{35}SO_4^{2-}$ per ml sample (corresponding to a total volume of ~5 µL per 10 ml sample). During the amendment, the stoppers were swiftly removed. To minimize contamination with oxygen during the procedure the vials were gently flushed with N_2, and an addition of 1 mM Na_2S (final concentration) was added to persevere reducing conditions. Microbial activity was terminated 2 hours after the radiotracer amendment (except for the first three time-points which were terminated 4 – 8 h after amendment) using 20 ml ZnAc (20%) and subsequently frozen at -20℃ until distillation. The Zn^{2+} also acts to precipitate the others volatile H_2S to solid ZnS.

*Table 3: Summary of experimental conditions during the SRR-experiment. **Na_2SO_4*

Experiment	*Incubation temp. range (°C)*	*Total incubation duration (h)*	*Culturing vial(s)*	*Basal media*	*SO_4^{2-} (mM)*	*Organic Substrates (final conc.)*	*Reducing agent (Na_2S final conc.)*
SRR	*50*	*96*	*Serum vials*	*Brackish water*	*28.2***	*Spirulina ~2.5 g/L* *Acetate 2.0 mM* *Propionate 2.0 mM* *Butyrate 4.0 mM* *Lactate 4.0 mM* *Formate 8.0 mM*	*1.0 mM*

3.5.1. Distillation

A cold chromium chloride-hydrochloric acid distillation was performed according to Kallmeyer et al. (2004). Information about preparations of chemicals can be found in Appendix B. The frozen samples were thawed for about two hours before separation of the $^{35}SO_4^{2-}$ containing supernatant from the TRIS (which was all insoluble after precipitation with Zn^{2+}). This was done by centrifuging the samples in 1811 rcf for 10 minutes. 0.1 ml of the supernatant was subsequently transferred to a plastic scintillation vial containing 0.9 ml mQ. 2.0 ml of liquid scintillation cocktail (UltimaGold, Perkin Elmer) was thereafter added, and the concoction was mixed thoroughly. Approximately 1.5 ml of the supernatant was set aside for later sulfate analysis using IC, and the rest was decanted and disposed as radioactive waste. The sediment pellet was transferred to a three-necked distillation flask preloaded with a magnetic stirring bar and two drops of antifoam. To minimize loss of sample (which sometimes was hard to remove since the consolidated sediment pellet was firmly attached to the centrifuge tube after centrifugation), the transfer was made by flushing with N,N dimethylformamide (DMF). Despite its toxicity, DMF was also considered necessary since it solubilizes elemental sulfur and destabilizes the stable S-S bonds, which thereafter facilitates reduction to sulfide by the reduced chromium chloride-hydrochloric acid solution (Kallmeyer et al., 2004). After transfer, the distillation flasks were connected to the distillation set-up (Fig. 5) consisting of a citrate trap containing 7.0 ml 0.1 M citrate solution (pH ca 4.0) and a ZnAc-trap containing 7.0 ml ZnAc (5%) and two drops of antifoam. The purpose of the citrate trap was to prevent aerosols to reach the final ZnAc-trap. All connections were secured with metal clamps to prevent gas leakage and the system was subsequently flushed with N_2 for 10 minutes to drive out oxygen. To convert the ZnS and FeS back to H_2S, 8.0 ml of HCl (6N) was added through a chemical port on the side of the distillation flask. This was followed by 16.0 ml reduced chromium chloride hydrochloric acid, which reduces FeS_2, S_0, and other partly oxidized sulfur species back to H_2S. The N_2-flow was adjusted to a bubbling rate (as seen inside the traps) of approximately 5 bubbles per second during the 2-hour long distillation time. Efficient break-up of the sediment pellet was secured by placing the distillation flask on a magnetic stirrer with a continuous stirring during the entire distillation. A sulfide carrier in the form of 1.0 ml of 1.0 mM Na_2S was added to the samples from station 23 and 50 to secure an adequate carry over of H_2S (it was apparent from the precipitated ZnS that the sulfide-content from station 13 and 14 did not require any addition of Na_2S). Over the last 20 minutes of the distillation period, the flow rate was increased to remove a potential last residue of sulfide. The entire content in the ZnAc-trap was thereafter transferred to plastic scintillation vials, and subsequently mixed with 14.0 ml scintillation cocktail. The workflow of the radiotracer method is summarized in Figure 6.

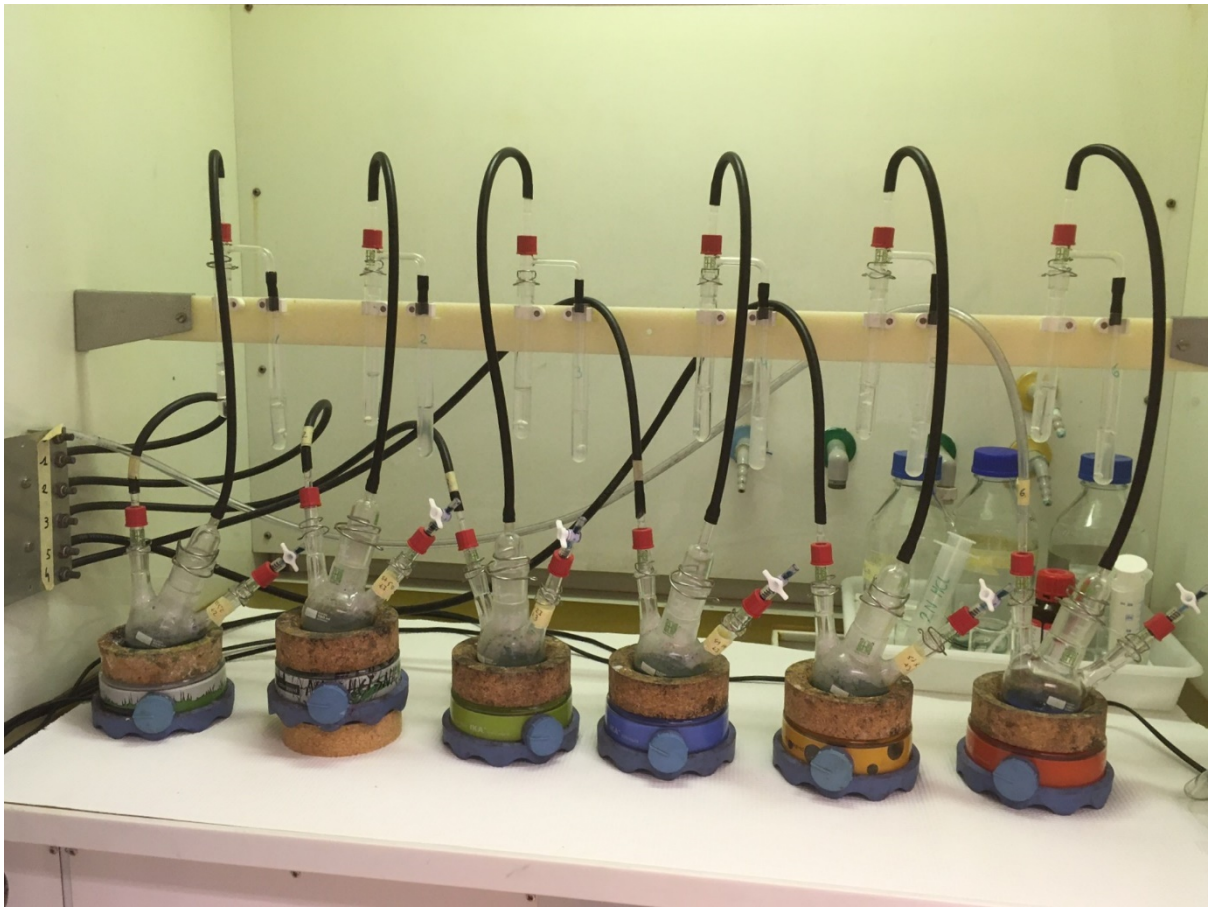

Figure 5: Distillation set-up of 6 samples.

3.5.1.1. Distillation efficiency

To test the efficiency of the distillation, a total of 6 control samples with known sulfide concentrations (1 mM Na_2S) were prepared and distilled beside the sample distillations. The concentration of sulfide in the distillate was analysed using spectrophotometry. Two to three counter blanks were also measured at each measuring event in the scintillation counter to measure the average background radioactivity. To test for potential contamination between distillations, as well as to assure that no radiolabelled sulfur compounds that have not been subject to bacterial DSR was carried over during the distillation, two sample blanks were prepared as follows: sediment samples prepared and incubated in parallel with the other samples were amended with 20 ml ZnAc (20%) to stop sulfate-reduction. $^{35}SO_4^{2-}$ were thereafter added in the same amount as used in the other samples. Since no sulfate-reduction should be present in the "killed" sediment samples, no radiolabelled TRIS should form and no increased radioactivity from the distilled samples should be detected by scintillation counting.

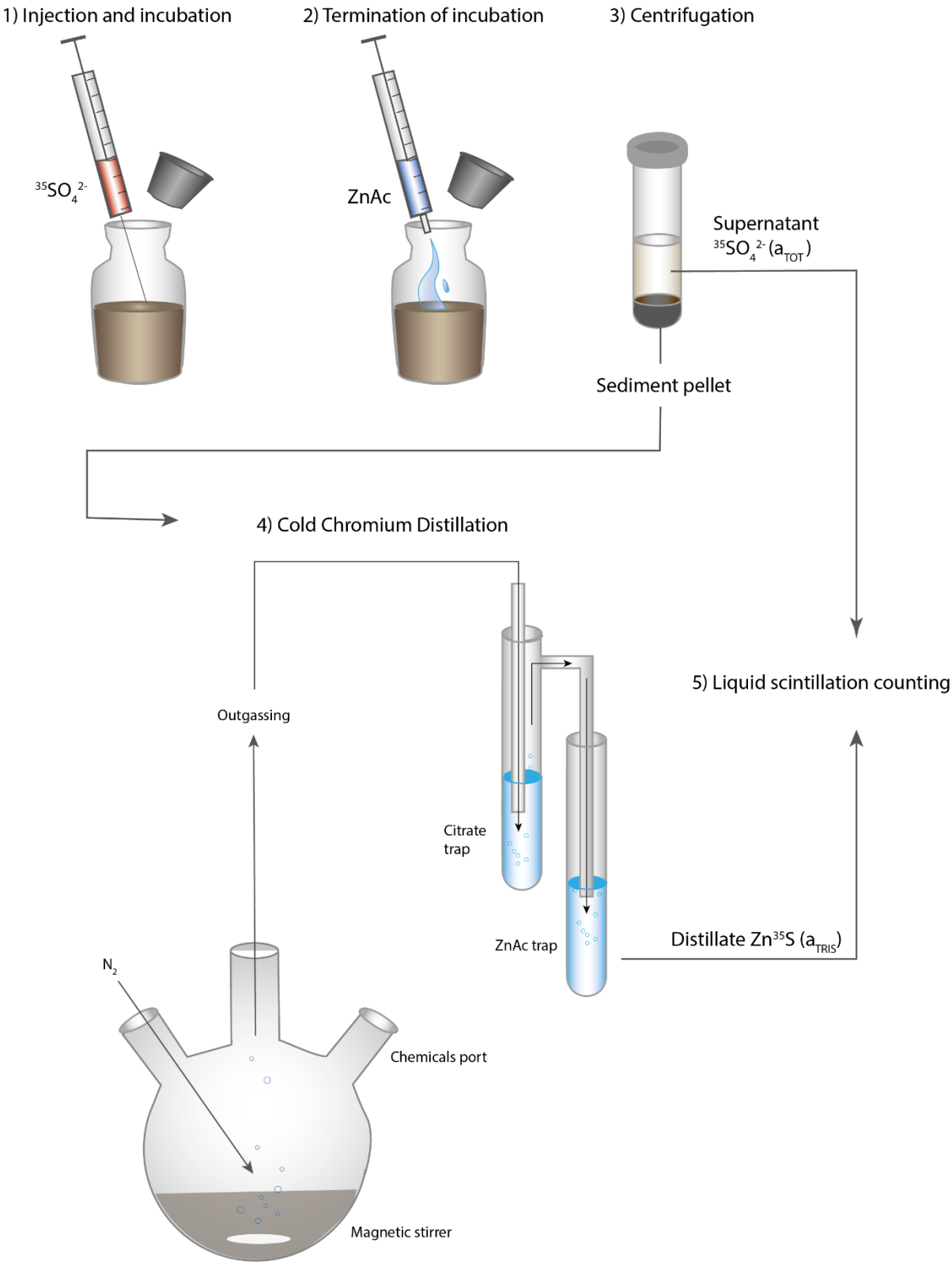

Figure 6: Workflow of the radiotracer method.

3.6. Analytical methods

3.6.1. Sulfate analysis

Sulfate concentrations were determined via IC using a Dionex Aquion. The TGE samples were initially analysed using a AERS 500 suppressor from Thermo Scientific. However, the suppressor was later changed (due to normal deterioration) and the sulfate analyses from the SRR experiment was instead made using a ADRS 600 suppressor. The column for measuring sulfate (together with other inorganic anions) was a AS22 Fast with the flow rate set to 1.2 ml/min. The eluent was 4.5 mM Na_2CO_3 / 1.4 mM $NaHCO_3$ (as specified by the manufacturer) and the injection loop was 25µl. The chromatograms were visualized using the Chromeleon Software (also from Thermo Scientific) and peak areas were calibrated using standard sulfate solutions made from Na_2SO_4. To verify the precision and accuracy of the instrument performance, several control samples with known concentration of 0.2 mM (CRM 3181) were measured at regular intervals at each measuring event. The uncertainty of the measured control samples was calculated to $\pm$ 2.5 µM, corresponding to a relative uncertainty of $\pm$ 1.2 %.

Prior to analysis, 20- to 62.5- fold dilutions of the samples were made. This was done to dilute the high salt concentrations (including sulfate), but also to dilute the Zn^{2+} concentration which otherwise can degrade the analytical column of the ion chromatograph (Røy et al., 2014).

3.6.2. Sulfide analysis

Sulfide concentrations in control experiments were determined by spectrophotometry as described by Cline (1969) using an Evolution 260 Bio-UV Visible spectrophotometer from ThermoFisher Scientific and associated software INSIGHT2 v2.1.133. Before analysing the samples, a calibration curve was constructed using a dilution series of a ZnS standard stock solution (1 mM) to concentrations ranging from approximately 0 to 40 µM ZnS. 10 ml of each concentration was mixed with 0.8 ml diamine mixed reagent and immediately capped to prevent volatilization of H_2S. After 30 min in the dark, 1 ml of the concoction was transferred to 1 ml cuvettes and measured at 670 nm in the spectrophotometer. A calibration curve was constructed with the absorption on the x-axis and the respective sulfide concentration on the y-axis. An absorption coefficient was then obtained by fitting a linear function to the data points, which subsequently could be used to calculate the concentrations from the absorbance of the measured samples, which were prepared in the same way as the standards as just described.

3.6.3. Scintillation counting

Beta emission was measured by liquid scintillation counting using a Tri-Carb 2910TR liquid scintillation counter and associated software Quanta Smart v4.0 from Perkin Elmer.

4. Results

4.1. Temperature gradient and time-series experiments

Temperature gradient experiments using media with different organic substrates and salt-concentrations (table 2) were designed to investigate temperature optima and salt-depending growth yields in sediments from the WGB. This was done to test if temperature and salt concentration could be used to select for different microbial communities adapted to a marine- or freshwater source habitat. Slight adjustments in experimental conditions (chosen temperature range, form of sulfate, incubation time etc.) between the different TGEs were made to figure out how to improve the overall cultivation method. Replicate samples were used to calculate the overall

uncertainty. For all TGEs and TSEs, the mean standard uncertainty was ± 0.2 mM with a minimum and maximum range between ± 0.1 to 0.4 mM and a median of ± 0.2 mM. In the graphs below (Fig. 7 to Fig. 10), changes in concentration of > 0.5 mM were considered of relevance and marked with grey boxes.

4.1.1. TGE #1

The results from TGE#1 are visualized in Figure 7a-d. After 48 hours at brackish conditions, approximately 1 mM drawdown of sulfate was observed within a temperature range of ca 31 to 54℃ (Fig. 7b). This thermophilic signal remained after 72h, and after 96 h the accumulated amount of reduced sulfate had increased to ca 3 mM (Fig. 7c,d). The temperature maximum at which a drawdown of sulfate were observed increased from 54 to ca 58℃. However, data retrieved after 96 h were noisy, as reflected in the saw-toothed pattern of sulfate concentrations in the temperature range where sulfate-reduction was presumed to be present (Fig. 7d).

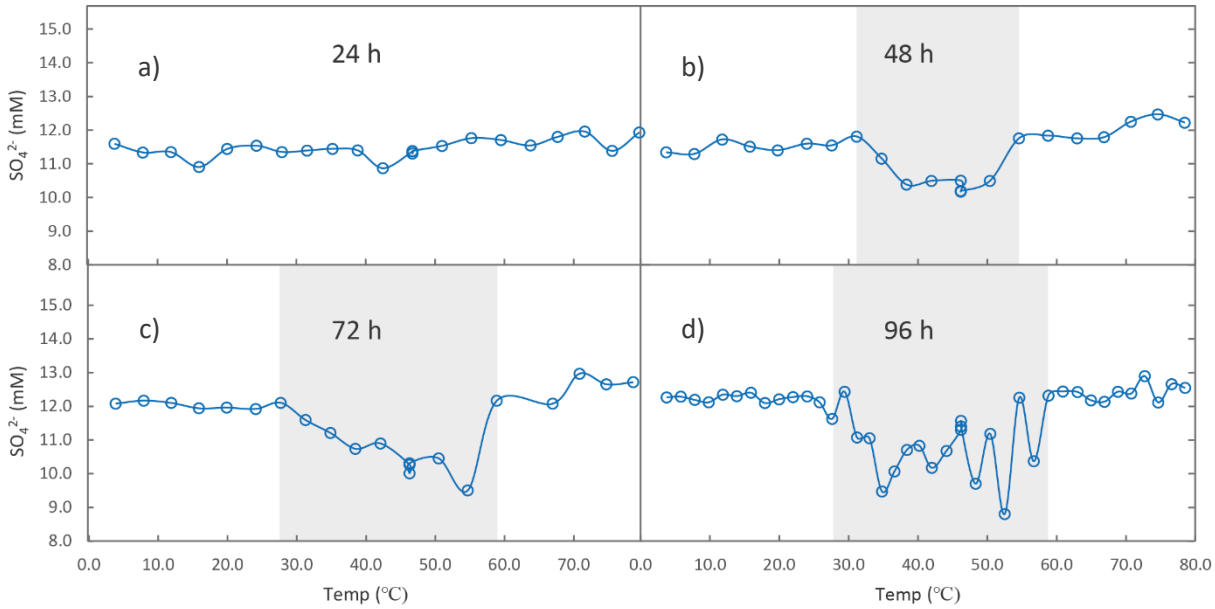

Figure 7: Results from TGE #1 showing sulfate concentrations over time in sediment slurries mixed with brackish media (SO_4^{2-} 8 mM) in a temperature gradient from ca 4 to 79℃. The shaded areas indicate drawdown of sulfate of > 0.5 mM.

4.1.2. TGE #2

In TGE #2, a mesophilic signal was observed in a temperature range between approximately 25 to 44℃ after 116 to 167 h in slurries mixed with saltwater media (Fig. 8a,b). A maximum drawdown of ca 4 mM sulfate occurred during the incubation. An interesting observation was that no drawdown of sulfate occurred above 45℃, in contrast to cultures grown using brackish water (i.e. TGE #1). This is also apparent when comparing time series from TGE #1 and #2 held around 50℃ (Fig. 9a,b). In the constructed time-series from TGE #1, there was a total drawdown of ca 3 mM after 96 h, whereas for the time-series in TGE #2 there was no apparent change in concentration during the entire incubation of 168 h.

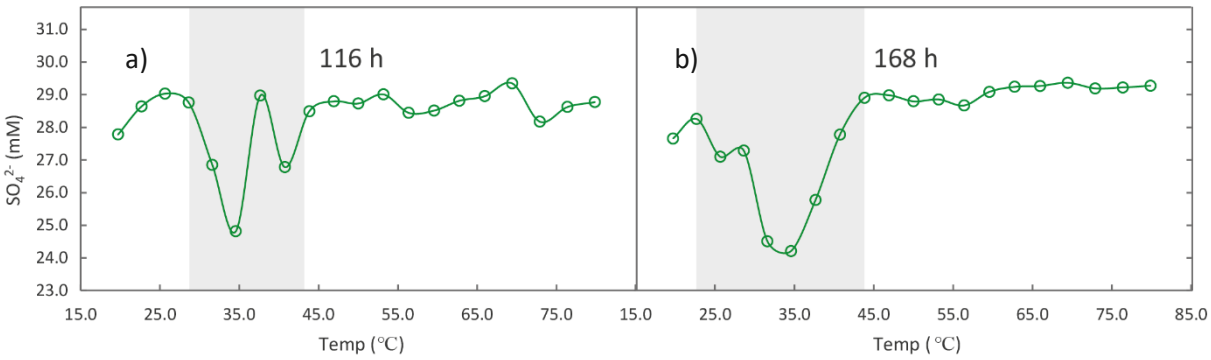

Figure 8: Results from TGE #2 showing sulfate concentrations after 116 h (a) and 168 h (b) in sediment slurries mixed with saltwater media (SO_4^{2-} 20 mM) incubated in temperatures ranging from ca 20 to 79℃. The shaded areas indicate a drawdown of sulfate of > 0.5 mM.

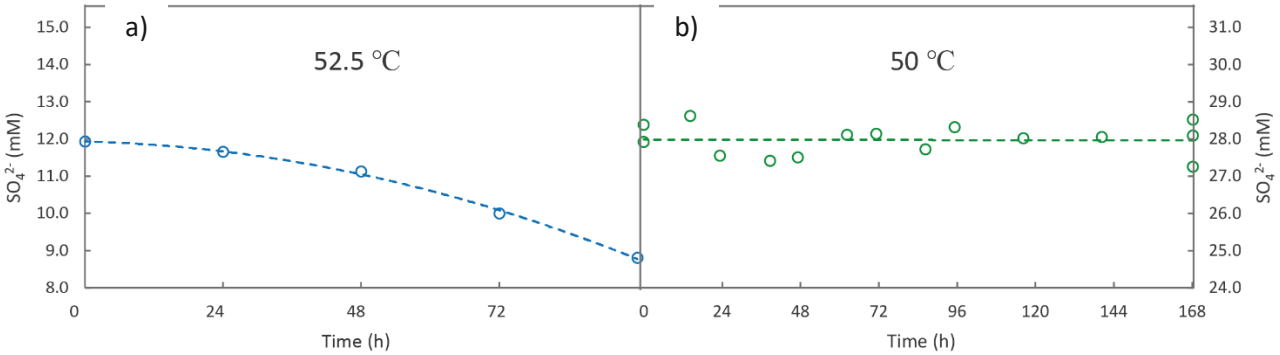

Figure 9: Sulfate concentrations over time from TGE #1 using slurries mixed with brackish media (a), and from TGE #2 using slurries mixed with saltwater media (b). Note the different sulfate concentrations on the y-axes.

4.1.3. TGE #3

TGE #3 repeated previous experiments using sediment slurries mixed with both fresh,- brackish-, and saltwater media (Fig. 10a,b,c). Anaerobic culturing vials of the Hungate-type were used instead of exetainers. The results were very noisy, and there was a noticeable increase in sulfate concentration with increasing temperatures (most notably in the samples using brackish media, Fig. b). A slight decrease in sulfate concentration appeared around 40, 50, and 65℃ in the freshwater-samples (Fig. 10a), around 25, 39, 57, and 65℃ in the brackish water-samples (Fig. 10b), and around 30 and 48℃ in the saltwater samples (Fig. 10c). However, the maximum drawdown of sulfate was only 0.5 to 1.5 mM. This was much lower than in TGE #1 and #2, which had a maximum drawdown of ~3 mM.

A diagnostic feature of sulfate-reduction is the blackening of samples upon sulfide production due to precipitation of FeS (Widdel&Bak, 1992). The decrease in sulfate concentration around 40 and 50℃ in the cultures mixed with freshwater media (Fig. 10a) co-occurred with samples turning black (samples f9 and f12 in Fig. 11), indicating sulfate-reduction and not due to some random noise.

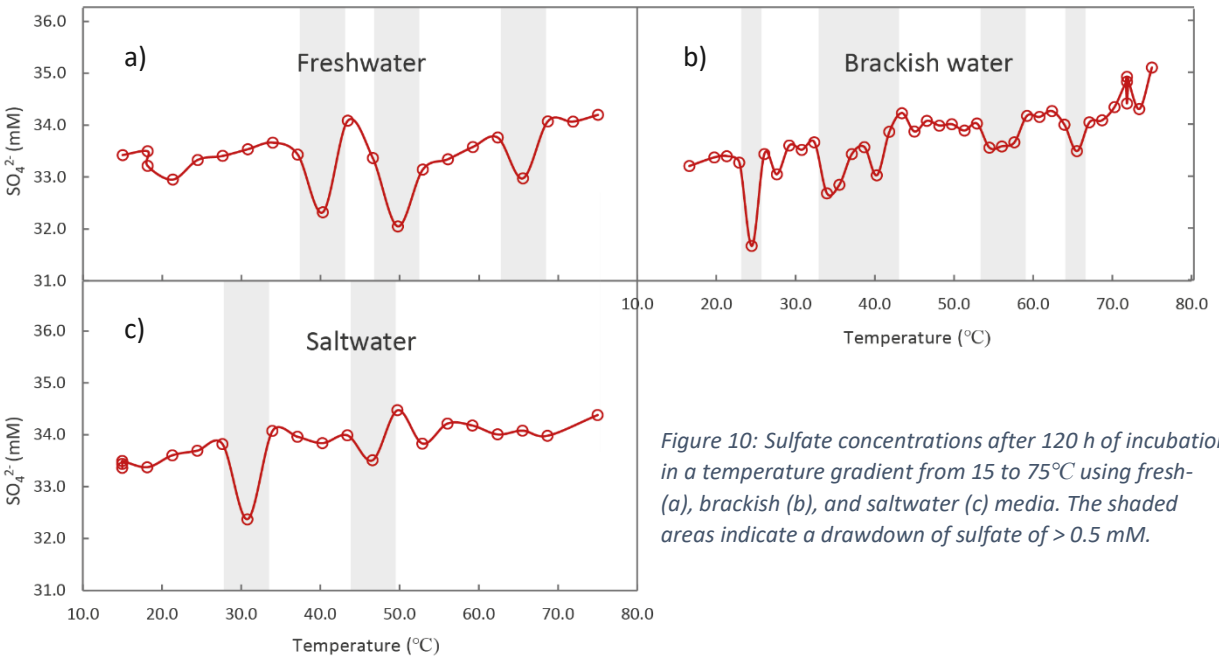

Figure 10: Sulfate concentrations after 120 h of incubation in a temperature gradient from 15 to 75℃ using fresh- (a), brackish (b), and saltwater (c) media. The shaded areas indicate a drawdown of sulfate of > 0.5 mM.

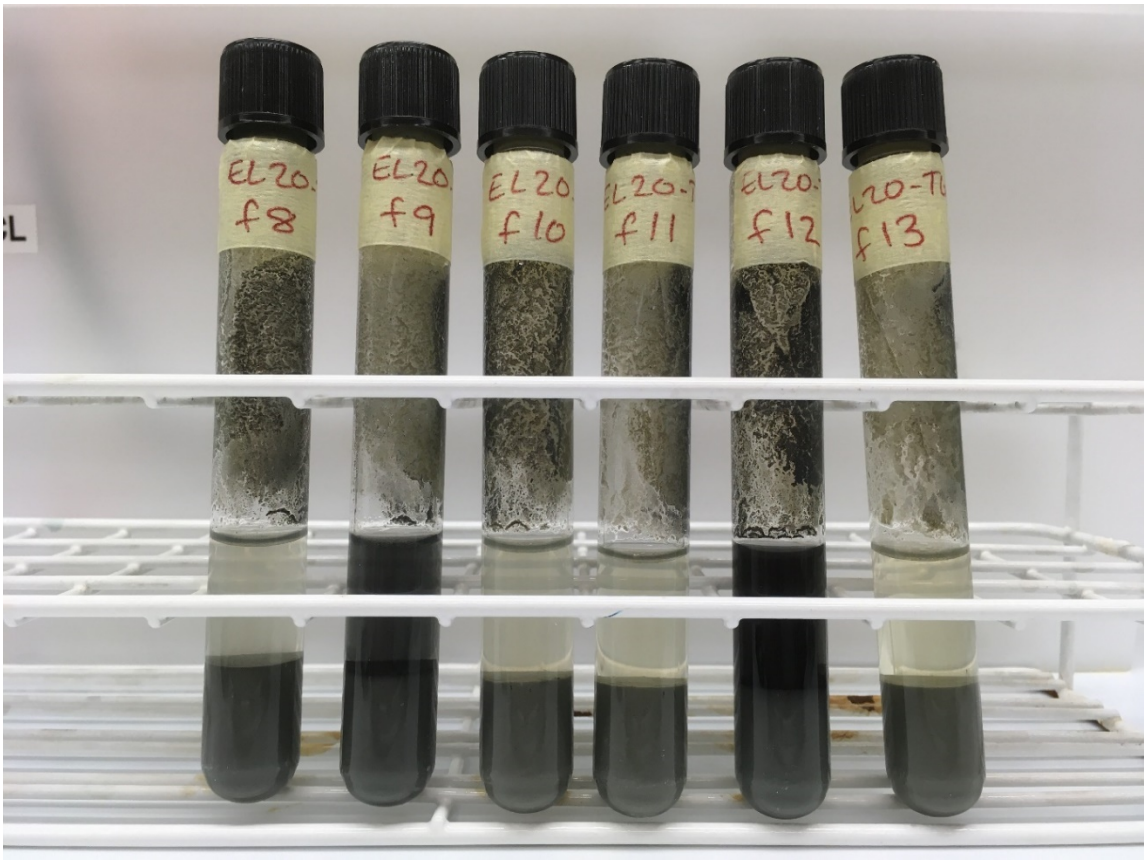

Figure 11: Freshwater samples (f8 to f13) corresponding to a temperature interval between 37 and 53℃ from TGE #3. Sample f9 (40℃) and f12 (50℃) have turned black, likely due to precipitation of FeS. The colour change co-occur with the decrease in sulfate concentration around 40 and 50℃ seen in Figure 10a.

4.1.4. TGE #4

TGE #4 repeated the above experiment with sediment slurries mixed with brackish water and the same amendments and concentrations as in TGE #3 (almost all sediment was used up and it was not possible to repeat the experiment with fresh- and saltwater as well). The Hungate-type culturing vials were changed back to exetainers as they had proven to be the best choice from conducted control experiments (see below). Improvements to the experimental design were made based on experiences during the previously conducted experiments, yet no apparent reduction was visible in TGE #4 (Fig. 12). The outlier at 68℃ was coincidental with a sample that had > 5% weight loss during the incubation time. Apart from that individual sample, there was no significant weight loss for the rest of the samples during the incubation time, but there was still a slight increase in concentration. However, the measured reference samples indicated an instrumental drift resulting in a maximum error of more than 1% during the measuring interval when the samples for TGE #4 were measured (Fig. 12).

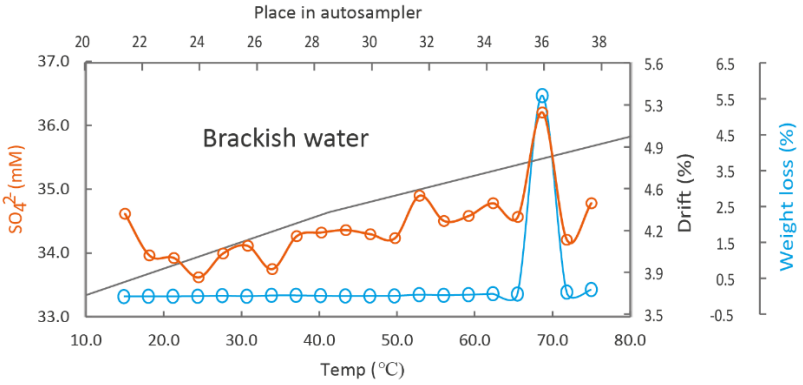

Figure 12: Results from TGE #4 using sediment mixed with a brackish medium. There is no apparent decrease in sulfate concentration. On the contrary, the concentrations show a slight increasing trend. This increase could be correlated with an instrumental drift of ca 1% during the time the samples were measured. The large spike in concentration at 68℃ co-occurred with a sample that lost > 5% of weight during the incubation time.

4.2. Control experiments

4.2.1. Vial control

In Figure 13a-d below, the shaded grey areas symbolize changes in the negative direction compared to the initial sulfate and sulfide concentration at the start of incubation. The sulfate concentration in culturing vials held at a constant temperature of 50℃ changed in both the Hungate tubes as well as in the exetainers (Fig. 13a). When using the Hungate tubes, there was a slight positive trend in concentration, with a large change of ca +0.5 mM after 96 h of incubation. For samples incubated using exetainers, the concentration in sulfate was rather stable apart for one dip in concentration of ca -0.5 mM after 24 h of incubation. However, there was no apparent correlation between the increased concentration in sulfate in the Hungate-tube and the sulfide concentration for the same sample, as would have been expected if sulfide was oxidized to sulfate due to contamination with oxygen. The concentration of sulfide dropped to below detection limit in both the Hungate tubes and the exetainers after 96 h of incubation (Fig. 13c). Sulfate concentrations in samples incubated in the TGB showed slightly more variations above than below 42℃ (Fig. 13b). The concentration in samples using exetainers was relatively stable, but there was a slight change of ca -0.3 mM between approximately 30 and 60℃. The negative trend changed at 65℃, at which point the only correlation between an increase in sulfate and a decrease in sulfide could be observed (Fig. 13a,c). For samples in the TGB using the Hungate tubes, the change in sulfate concentration was both in the positive and

negative direction, most notably the change of ca 1 mM around 50℃. There was no correlation with the sulfide concentration in the same sample, however (Fig. 13b,d). The sulfide concentrations in the Hungate tubes were in fact relatively stable (apart from the dip around 33℃). In contrast to the Hungate samples, the samples from the exetainers showed large variations in sulfide concentration. Furthermore, the variations were always in the negative direction with a maximum change of -0.7 mM (Fig. 13d).

The samples were also weighed regularly to monitor the potential weight loss. As clearly can be seen in Figure 14, the Hungate tubes lost most weight. More than 1.2% of weight loss had occurred after 120 h in samples incubated at 75℃, opposed to a modest loss of 0.07% in the exetainers.

In summary, the largest changes in sulfate concentrations seemed to occur for samples incubated using Hungate tubes. The change in concentration mainly occurred in the positive direction with a maximum change of almost +0.9 mM. Exetainers had relatively stable sulfate concentrations compared to the Hungate tubes, with a maximum change of -0.6 mM. The changes in sulfide mainly occurred in the negative direction, with largest change occurring in the exetainers with a decrease of 0.7 mM. The concentration in the Hungate tubes (apart from one single dip) was generally less than 0.3 mM in the negative direction. The weight loss in exetainers was considerably lower than for the Hungate tubes. The weight loss in the Hungate tubes likely explains the observed increasing trend in sulfate concentrations. However, there was no corresponding increase in sulfide concentrations, which would have been expected if there was no loss of sulfide.

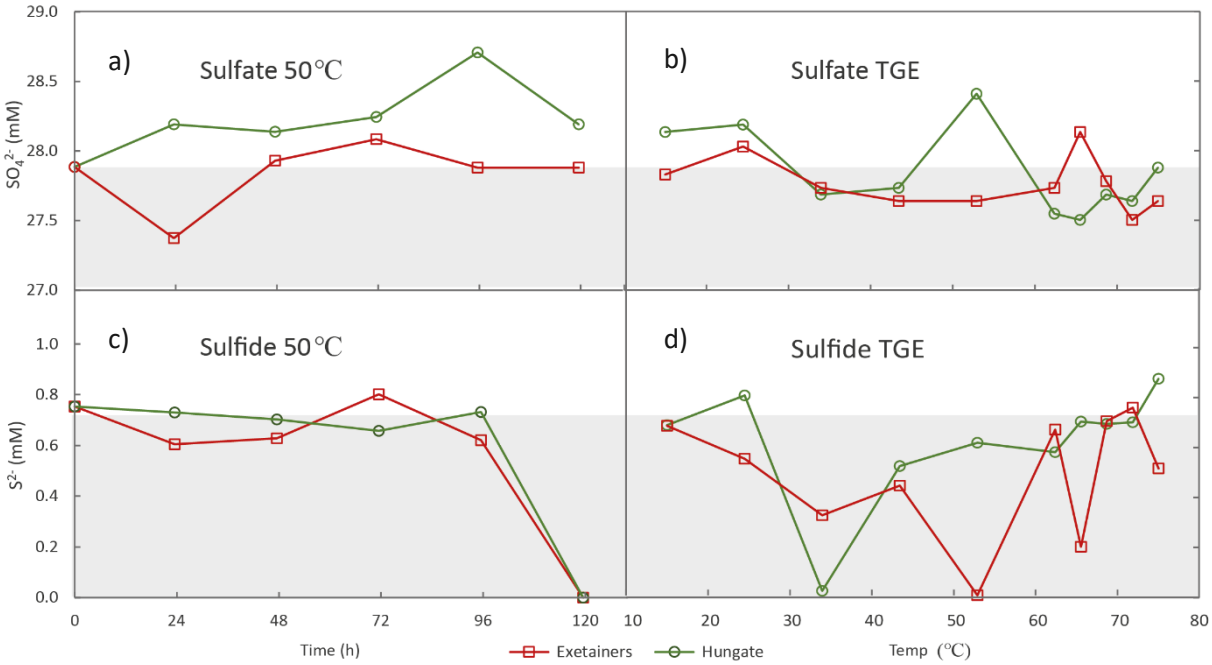

Figure 13: The panels to the left show sulfate (a) and sulfide (c) concentrations over time in samples incubated at a constant temperature of 50℃ for 120 h. The Panels to the right show sulfate (b) and sulfide (d) concentrations in samples incubated for 120 h in a temperature-gradient between 15 and 75℃.

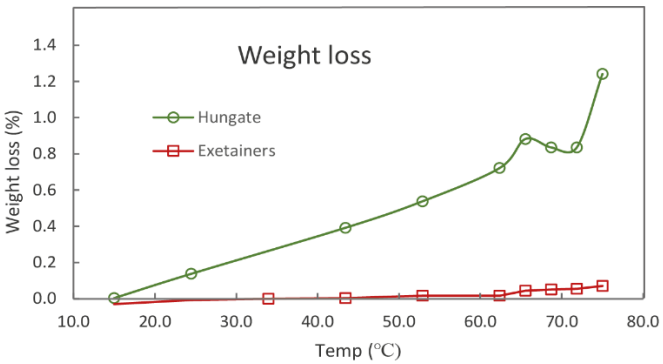

Figure 14: Monitored loss of sample weight in samples incubated in a temperature gradient between 15 and 75°C.

4.2.2. Media control

Comparisons between cultivation media containing different organic substrates, with or without a reducing agent (Na_2S), are presented in Table 4. The lowest amount of accumulated reduced sulfate (5.7 mM) was found in samples containing only *Spirulina*. The samples containing additional VFAs decreased about 1 mM more compared to the samples containing only *Spirulina*. However, the highest drawdown of sulfate (7.4 mM) was found in the samples amended with both *Spirulina*, additional VFAs, as well as a reducing agent. In these samples the total drawdown of sulfate was 1.7 mM more compared to using only *Spirulina* and no reducing agent.

Table 4: A comparison between cultivation media amended with different organic substrates and with or without a reducing agent.

Amendment	**SO_4^{2-} (mM) at start**	**SO_4^{2-} (mM) at end**	**Accumulated SO_4^{2-} reduced (mM)**
Spirulina	10.9	5.3	5.7
***Spirulina*, VFAs**	11.0	4.4	6.6
***Spirulina*, VFAs, and reducing agent**	10.9	3.5	7.4

4.2. Sulfate-reduction rates

Sulfate concentration

The calculated uncertainty from replicate samples in the SRR experiments gave considerable higher uncertainties in sulfate concentrations compared to the TGEs. The mean uncertainty for all stations was calculated to ± 0.6 mM, with a range from ± 0.1 to 2.8 mM and a median of ± 0.3 mM. Station 13 was the only station with a noticeable decrease in accumulated reduced sulfate, with a lowering from an initial ~20 mM to less than 12 mM after 96 h. Furthermore, there was a rapid drop of ca 10 mM during the last day of the incubation between 96 and 120 h (Fig. 15a). A barely noticeable decrease was seen in sulfate concentrations from station 14 (Fig. 15b).

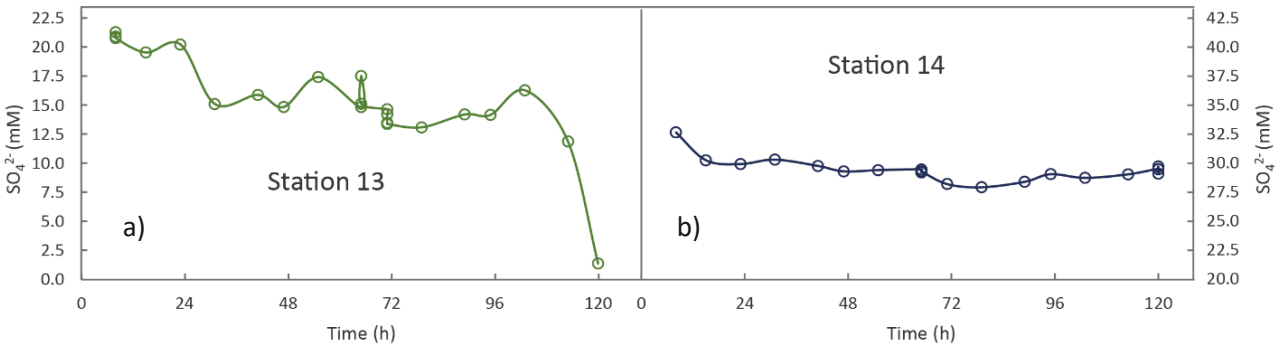

Figure 15: Sulfate concentration in radiolabelled incubations from station 13 (a) and 14 (b) held at 50°C.

Distillation efficiency

The efficiency of the distillation was estimated as described in section 3.5.1.1. In distilled control samples, a mean of 96% of the total sulfide was recovered. The distilled sample blanks showed no carryover of sulfide (measured radioactivity in the distillate did not have higher radioactivity compared to the counter blanks). For SRR to be detected, the produced TRIS must have a higher radioactivity than the sample and counter blanks. A detection limit for SRR under the prevailing conditions was estimated based on an average value for the sample blanks (25 cpm) and the measured total activity in the samples (19703528 cpm). An average detection limit for an incubation time of 2 h was subsequently calculated by inserting the numbers into Eq. 1. The obtained result indicated that a SRR > 0.02 nmol cell^{-1} h^{-1} must be present to produce sufficient amounts of TRIS.

Calculation of SRR

The measured radioactivity from the distillate (a_{TRIS}) and the supernatant ($a_{sulfate}$) was used to calculate SRRs according to Eq. 1. Active sulfate-reduction could be detected at station 13 and 14, whereas station 23 and 50 had no SRR above the detection limit. Most of the calculated SRRs at station 14 were barely over the estimated detection limit. Relative uncertainties were estimated to facilitate comparisons between the large range of the calculated SRRs, and was based on replicate samples that had a SRR above detection limit. Only one set of replicates met this criterium from station 14, which had a relative uncertainty of ± 58%. The relative uncertainty from station 13 was calculated to a mean of ± 34%, with a range between ± 27 to 42%. Despite the high uncertainties, distinct growth phases were clearly present in the constructed growth curves from station 13 and 14 (Fig. 16a,b). The first exponential phase at station 14 occurred after 48 h. The highest SRR of 0.13 nmol cell^{-1} h^{-1} peaked after ca 56 to 72 hours of incubation. Another peak in SRR seemed to occur after 104 to 120 h, but even the highest SRR around this time was below detection limit and the results were thus highly questionable (Fig. 16b). Two exponential growth phases were seen at station 13, occurring after 16 and 88 h, respectively (Fig. 16a). The highest SRR at station 13 was more than 1000-fold higher than at station 14, with the highest rate amounting to 222 nmol cell^{-1} h^{-1} around 32 h of incubation. A similar pattern for the growth curves at both station 13 and 14 was that the exponential growth rapidly abated after reaching the maximum SRR.

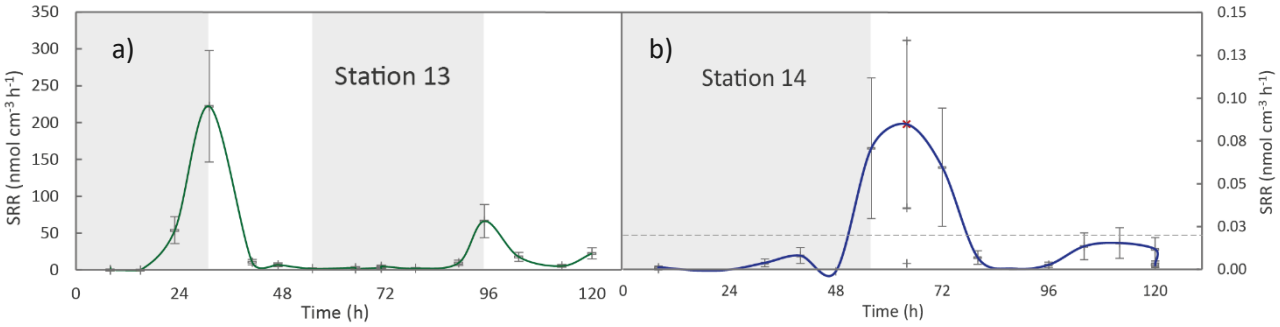

Figure 16: The growth curve from station 13 (a) shows two distinct growth phases after 16 and 88 h. The error bars show the uncertainty of ± 34%. The growth curve from station 14 (b) shows one distinct growth phase after 48 h of incubation, and one potential phase just below detection limit after ca 96 h of incubation. The broken line just above the x-axis shows the estimated detection limit. The red cross is a mean value calculated from replicate samples with a large range in estimated SRRs. The error bars indicate the uncertainty of ± 58%. The shaded areas indicate the exponential phases from which exponential functions were fitted (compare to Figure 17a,b).

Estimation of initial numbers of endospores from tSRB

Estimations of initial numbers of endospores were done using an approach described by de Rezende et al. (2017). Exponential functions were fitted to calculated SRRs from the time-intervals where exponential growth was detected (shaded areas in Fig. 16a,b). The two growth phases seen in Figure 16a from station 13 were treated separately. The resulting functions (Fig. 17a,b) are in the form of Equation 4, which reflects the exponential increase in SRR due to an exponentially growing microbial population (compare to Eq. 3 in 2.5.3.).

$$SRR(t) = SRR_0 \times e^{kt} \qquad \textit{Eq. 4}$$

The function allowed the SRR to be estimated at any time point (t) during the experiment. Furthermore, the function was used to estimate the doubling time during exponential growth (T_2) from the obtained value for the specific growth rate (k): $T_2 = ln(2) \times k^{-1}$. The function was also used to estimate the initial SRR (SRR_0). Under the assumption that all endospores germinated at time zero (t0), the obtained SRR_0 values were used to estimate the initial numbers of endospores. Before this could be calculated however, the cell-specific SRR (csSRR) had to be known known.

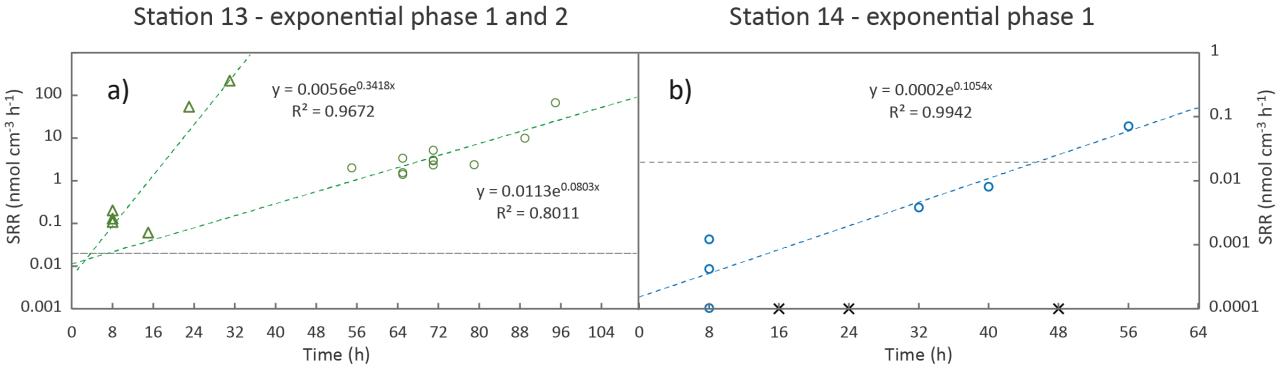

Figure 17: Two exponential growth phases with corresponding exponential functions from station 13 (a), and one exponential growth phase with corresponding exponential function from station 14. The crosses at 16, 24, and 48 h correspond to samples with a_{TRIS} < sample blanks, which results in erroneous negative values (b). The broken horizontal lines coloured in grey represent the detection limit.

Values for csSRR can be obtained from the literature, but here another approach (also presented by de Rezende et al. 2017) was used by pursuing Equations 5 to 7:

By integrating Equation 4, the accumulated amount of reduced sulfate was calculated according to Equation 5:

$$SO_4^{2-}reduced = SRR_0 \times \frac{1}{k} \times e^{kt} \qquad \textit{Eq. 5}$$

The accumulated amount of reduced sulfate (in nmol) was then multiplied by the growth yield (i.e. the biomass produced per nmol reduced sulfate, pg nmol^{-1}) according to Equation 6, providing an estimate of the total amount of biomass produced (in pg):

$$Total\ biomass\ produced = SRR_0 \times \frac{1}{k} \times e^{kt} \times Y_{sulfate} \qquad \textit{Eq. 6}$$

where $Y_{sulfate}$ is the growth yield. Dividing the total amount of biomass produced by the amount of biomass contained in one cell (bm_{cell}, in pg cell^{-1}) finally gave the numbers of vegetative cells during the time of interest (i.e. the number of endospores at t0):

$$Number\ of\ cells = SRR_0 \times \frac{1}{k} \times e^{kt} \times \frac{Y_{sulfate}}{bm_{cell}} \qquad \textit{Eq. 7}$$

The same numbers for $Y_{sulfate}$ (8200 pg nmol^{-1}) and bm_{cell} (0.3 pg cell^{-1}) given in de Rezende et al. (2017) was used, such that it would be easier to compare the obtained results. But similar values for growth yields of *Desulfotomaculum* spp. can be found in the literature (ex by Cypionka&Pfennig, 1986). With the estimated csSRR the numbers of endospores at t0 were estimated by dividing the SRR_0 by the csSRR. All the results are presented in table 5 below.

Table 5: Summary of parameters obtained by the exponential functions that were fitted to the identified exponential growth phases, as well as calculated parameters obtained by following the calculation steps presented in Eq. 4 to 7.

Station / Exponential phase	**SRR_0** (10^{-3} nmol cm^{-3} h^{-1})	**k** (h^{-1})	**T_2** (h)	**csSRR** (fmol cell^{-1} h^{-1})	**Estimated nr of spores from tSRB at t=0**
Station 13 / 1	*5.6 (3.7 – 7.6)*	*0.34*	*2.0*	*12.5 (7.6 – 17.4)*	*448 (296 – 608)*
Station 13 / 2	*11.3 (7.5 – 15.1)*	*0.08*	*8.6*	*2.9 (1.8 – 4.1)*	*3846 (2553 – 5140)*
Station 14 / 1	*0.2 (0.1 – 0.3)*	*0.11*	*6.6*	*3.9 (1.6 – 6.1)*	*52 (22 – 82)*

5. Discussion

5.1. Endospores in the WGB, Laptev Sea, and the ESAS

Both the Baltic Sea and the Arctic Ocean are relatively isolated from the global ocean circulation due to a complex bathymetry with several sills acting as efficient barriers (Hanson et al., 2019). Moreover, the increased inflow of freshwater from rivers and melting ice during summer and sea-ice and brine formation during winter, creates a seasonally dynamic stratification and circulation pattern in these areas (Meier&Kauker, 2003; Anderson et al., 2017). Despite being relatively isolated from the global ocean circulation, the results from this study clearly indicate that germination and growth of endospores of tSRB in Baltic and Siberian shelf sediments were induced by incubating pasteurized sediment at elevated temperatures.

The two growth phases that can be observed at station 13 (and possibly at station 14) in the Laptev Sea probably reflects two distinct microbial communities, one slow-growing and one rapid-growing group. This is similar to what has been found in other studies concerning tSRB in the cold marine seabed (Isaksen et al., 1994; Hubert et al., 2009; de Rezende et al., 2013; 2017; Müller et al., 2014). Furhermore, the calculated parameters (Table 5) are in accordance with those estimated by de Rezende et al. (2017), who estimated almost identical values for *k* (0.34 and 0.09 h^{-1}) and T_2 (2 and 7.5 h) and only slightly different values for SRR_0 (2.2 and 34.7 x 10^{-3} nmol cm^{-3} h^{-1} sediment slurry). Moreover, the estimated csSRR of 2.9 and 12.5 fmol $cell^{-1}$ h^{-1} for the slower- and faster growing group, respectively, are in good agreement with what has been previously reported for SRB (Detmers et al., 2001). This validates the obtained results despite the high uncertainties. Interestingly, it was a large difference in SRR as well as in estimated endospore abundance between stations. Despite station 13, 14, and 23 being located within ~13 km from each other, no microbial activity was detected at station 23, and only a low SRR of a maximum of ~0.13 nmol cm^{-3} h^{-1} was present at station 14, compared to ~225 nmol cm^{-3} h^{-1} at station 13. Neither could any microbial activity be found at station 50, located ~80 km from the other stations. Moreover, the estimated endospore abundance was considerably lower at station 14 (~52 endospores per ml slurry) compared to station 13 (~3846 endospores per ml slurry). Assuming a sedimentation rate of ca 0.5 cm/year in the Laptev Sea (Bauch et al., 2001), the samples from station 13 and 14 consisted of 11 years of sediment (0 – 5.5 cm depth) and 8 years of sediment (2 – 6 cm depth), respectively. Considering that station 13 had ~3846 spores per ml slurry, and that the slurry consisted of 2 parts medium and 1 part sediment, the "true" abundance would be ~11 538 endospores cm^{-3} (on an average of 11 years). This means an abundance of ca 1049 spores cm^{-3} y^{-1}, or that ca 5.2 x 10^6 spores m^{-2} must have been delivered to the sediment each year to explain this number. For station 14, an estimate of 9.8 x 10^4 endospores m^{-2} must have been delivered each year. This is two and four orders of magnitude lower than what has been found in Svalbard sediments (Hubert et al., 2009, de Rezende et al., 2017). Even if there are large uncertainties associated with the estimated SRR and the abundance of endospores between stations 13 and 14 (as well as compared to the Svalbard sediments), the difference in magnitude is still unequivocal. The reason to the large difference in endospore abundance can only be speculated upon, but may be attributed to one or several of following explanations: i) *dispersal limitation* ii) *a recent emergence of endospores,* and/or iii) *the endospores are not viable or failed to germinate and grow*.

i) Dispersal limitation

The difference in abundance between Svalbard sediments (2 X 10^8 endospores m^{-2} y^{-1}, Hubert et al., 2009), station 13 (5.2 x 10^6), and station 14 (9.8 x 10^4) may be explained by dispersal limitation. In a study by Müller et al. (2014), it was recognized that locations with restricted ocean circulation contained lower phylotype richness as well as different microbial compositions compared to locations not isolated from global ocean circulation, suggesting that passive dispersal is largely dependent on the connectivity between water masses (Müller et al., 2014). On the contrary, long distance dispersal was inferred from the discovery that sediment from distant locations such as Aarhus Bay and Svalbard contained closely related species of *Desulfotomaculum*, which led to the conclusion that some, so called ‘‘cosmopolitan’’ species, have the potential to be dispersed over very long distances (de Rezende et al., 2013), which was also concluded by Müller et al. (2014). There are no coastlines or other bathymetric barriers in the flat shelf area of the Laptev Sea and East Siberian Sea that can explain a limited dispersal between the stations. However, it is more than 2000 km from Svalbard, and as illustrated by Figure 18, such a long distance may be well enough to explain a lower number of endospores in ESAS sediments compared to Svalbard sediments. Yet, it does not explain why it is such a big difference between adjacent stations. One possibility is that dispersal is limited due to separated water masses, for example by stratification of the water column. The water column in the area where station 13, 14, and 23 are located have previously been shown to be stratified (Baranov et al., 2020), and it is also recognized that there exist a water mass-specificity in bacterial community compositions (Agogué et al., 2011; Korneeva et al., 2015). Hence, it is possible that a stratified water column could limit endospore dispersal. However, this would likely limit dispersal in the vertical direction only, and not in the horizontal direction. Local circulation patterns may also explain the lack of endospores at adjacent stations. If the source of endospores came from, or close to, station 13, the voluminous input of riverine water could have transferred most of the endospores towards the deeper basin, instead of eastwards towards station 14 and 50.

ii) Recent emergence of endospores

A meager flux may be another reason explaining why such low numbers were found at adjacent stations. As mentioned in the beginning, the source habitat must have a sufficient magnitude to supply the surrounding sediments with a large number of endospores, particularly if they are to be detected at a large distance away from the source (Hubert et al., 2009; de Rezende et al., 2013). Another explanation is that the supply of endospores appeared more recently, and that the time necessary to deliver a multitude of endospores to more distant locations has not been long enough. Since the upper 2 cm from station 14 was absent, a recent emergence could explain ‘‘the missing endospores’’ since a corresponding 4 years of sediment was lost. Assuming a local source (likely sources will be discussed below), a recent appearance could be explained by melting permafrost. Permafrost is an effective barrier to the upward flux of gas. Degrading permafrost could thus create conduits in the sediment through which gas could migrate. Reactivation of faults and/or rifts could also create possible conduits for upward migrating gas (Baranov et al., 2020), and provide possible pathways for hitch-hiking endospores originating from a deep reservoir (Fig. 18) (Hubert&Judd, 2010).

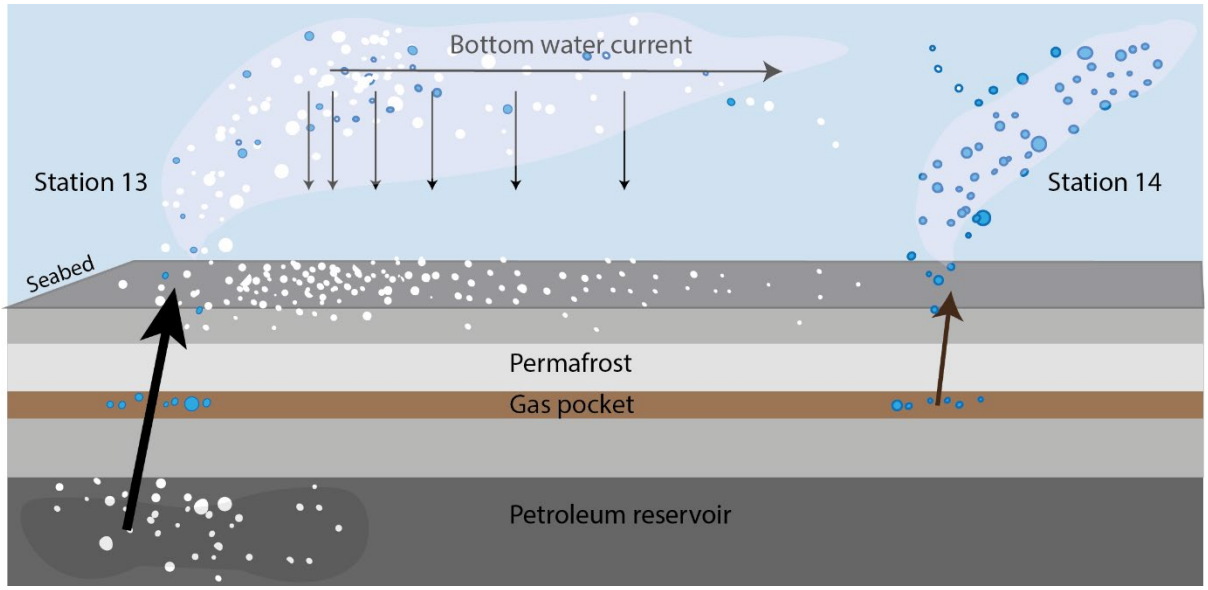

Figure 18: The figure illustrates the difference in endospore (depicted as white dots) abundance with distance. The further away from the source, the less endospores will be found in the sediment. The illustration also shows the interpretation of how endospores originating from a deep petroleum reservoir are ''hitch-hiking'' with upward emigrating gas, potentially through conduits created by faulting. The expelled endospores are subsequently carried away by currents. The gas from station 14 however, is thought to originate from a shallower source, for instance from gas pockets trapped beneath the permafrost. At places where the permafrost has degraded, conduits are formed which generates pathways for the upward emigrating gas. Adapted from Hubert&Judd, 2010.

iii) Non-viable endospores and failure to germinate and grow

Yet another explanation to the observed differences in endospore abundance, is that the endospores were non-viable due to a pro-longed storage time. In the work performed by Hubert et al. (2009) and de Rezende et al. (2017), experiments were performed in close association to sediment retrieval, whereas the sediment used in this project had been stored for 7 years. However, as was discussed in section 2.1.1., endospores are resilient structures, and it seems unlikely that they would have lost viability even during a 7 year-long storage. But, as will be discussed in section 5.4 below, it is highly likely that some endospores germinated prior to pasteurization, and subsequently perished during this sublethal heat-treatment. Uncertainties in estimated endospore abundance associated with the cultivation technique is further discussed below.

5.2. Endospores as an oceanographic tracer

To use endospores as oceanographic tracers, their source habitat and dispersal vectors must be identified. It was hypothesized, that if the temperature optima and/or the amount of reduced sulfate in incubated sediment-slurries with different salt-concentrations change (as detected by a change in the accumulated amount of reduced sulfate), it may imply that different microbial communities adapted to different environmental conditions develop depending on salt-concentration. If so, media with different salt-concentrations could be used to differentiate between source environments (i.e. a marine or terrestrial source), enabling their dispersal by ocean currents to be inferred, i.e. they could be used as an oceanographic tracer. Thus, endospore diversity was tested by inducing growth in a temperature gradient using sediments mixed with media of different salt concentrations. The results showed that optimal temperature where growth was induced varied depending on the chosen salt-concentration. For sediment mixed with freshwater media, optimal growth occurred around 40 and 50℃. Potential growth around 65℃ was possibly also present (Fig. 10a). For sediment mixed with brackish water, a broader range in temperature between ca 30 to

58℃ induced growth (Fig. 7 and Fig. 10b). When saltwater was used however, there was no indication of growth above 50℃ (Fig. 8, Fig. 9b and Fig. 10c).

In previous research by Isaksen et al. (1994) and de Rezende et al. (2017), it has been shown that sediments from Aarhus Bay harbour endospores originating from both terrestrial and marine sources. However, their presence has only been inferred using brackish- or saltwater concentrations, thus omitting germination and growth of freshwater species not capable of growth in saline conditions. Nevertheless, they found two temperature optima occurring around 40 and 60℃ (Isaksen et al., 1995), and around 45 to 60℃ with range of ca 28 to 70℃ (de Rezende et al (2013). In a recent investigation from the more closely located Landsorts Deep (located in the WGB), mesophilic endospore-forming SRB were isolated and induced to grow using freshwater medium. Optimal growth occurred at 20℃ (temperatures > 45℃ were not tested) with NaCl concentrations between 0 – 3.5%. In another study by Bell et al. (2018), growth experiments were designed to investigate the distribution of endospores of tSRB in estuarine sediments (River Tyne). Sediment was mixed with brackish- and saltwater media, and it was found that endospores were derived from both terrestrial and marine sources. Abundance estimates were also conducted, however only media with brackish concentrations were used for these essays, and it was hypothesized that greater number of endospores adapted to freshwater sources may have developed if lower salinities had been used. Moreover, the growth experiments were incubated at a constant temperature of 50℃ (Bell et al., 2018), which therefore excluded all tSRB having other temperature preferences.

These findings, together with the results from this study, show that the temperature optima in which growth seems to occur varies between experiments using media with different salt concentrations. However, there is an overlap between the salt-dependent temperature response. Especially growth media using brackish salt concentrations show a very broad temperature range in which growth is induced. This indicates that tSRB have a metabolic flexibility for growth under both fresh-, brackish-, and marine conditions, which makes it hard to use temperature and salt-concentration as the only mean to differentiate between microbial communities such that their source habitat (marine/terrestrial) can be inferred. However, not all species are equally tolerant for different temperatures and salinities, and as already mentioned there is no one media that suits all kinds of tSRB (Widdel&Bak, 1992). Therefore, it must be highlighted that the choice of cultivation conditions may exclude certain species not adapted to the temperature and salinity of choice. This implies that as long as cultivation-dependent methods are necessary, it is unavoidable that not all endospores from tSRB will germinate and grow. Hence, if endospores are to be used as a tracer, we must either presume a likely source habitat before cultivation (such that we can chose the best cultivation media for successful germination and growth), or we must look for cultivation-independent methods for their identification. Without further investigations it is therefore not possible to determine whether the endospores in sediments from the WGB are of a marine source originating and dispersed by Atlantic water masses, or of a terrestrial source dispersed with for example riverine water. As such, their origin as well as dispersal history remain elusive.

5.3. Endospores as bioindicators for hydrocarbon seeps

The shelves of the Laptev Sea and ESAS harbour vast amounts of carbon stored as gas hydrates, subsea permafrost, and deep reservoirs of thermogenic gas. In the wake of anthropogenic warming, an increasing concern has risen about how much methane these different subsea sources hold and how much they could contribute to amplify future global warming. Another important question is if the different pools will release methane gradually (for example as methane released from microbial

degradation in shallow sediments), or rapidly from pools with preformed methane (such as methane hydrates and reservoirs with thermogenic gas) (Steinbach et al., 2021). Currently, there are two major hypotheses concerning the observed methane release in the shelf sediments of ESAS; one that considers thawing permafrost and the dissociation of gas hydrates as the major source, whereas the other suggests deeper reservoirs of thermogenic gas as the prior source (Cramer&Franke, 2005; Baranov et al., 2020). As was discussed in section 5.1. the source providing endospores to the sediments at station 13 and 14 was probably closely situated to station 13. It has previously been found that Atlantic Ocean water contains low endospore abundances, probably reflecting limited sources in this region and a restricted connectivity to other oceans (Müller et al., 2014). What then could possibly be a local warm source habitat in the cold Arctic Ocean? One such source could be hydrothermal fluids expelled at the Gakkel Ridge, which, although being an ultra-slow spreading ridge, still hosts several active vent systems (Edmonds et al., 2003). A more closely associated source with an ephemeral character (opposed to hydrothermal venting) is even more likely to explain the large difference between station 13 and 14, however. Such a source could be a hydrocarbon seep. As was discussed in section 2.3.2., oil and gas reservoirs in the deep sediment may be potential source habitats for tSRBs (Hubert et al., 2009; de Rezende et al., 2013). The upward emigration and subsequent expulsion of gas and ‘‘hitch-hiking’’ endospores may thus explain the presence of endospores at station 13. In a recent work by Steinbach et al. (2021), it was shown by stable isotope fingerprinting that methane escaping the seabed at station 13 likely originated from a thermogenic source, whereas the signature from station 14 indicated a mixed source of possible thermogenic and microbial origin (illustrated in Fig. 18) (Steinbach et al., 2021). The sediment from station 23 and station 50, which were chosen as reference stations with no indication of methane seeping from the seafloor, did not show any sign of containing endospores. As has been stated above, without identification, the true source to these endospores can only be speculated, but the presence of such indigenous microorganisms at station 13, and the co-occurrence with a strong thermogenic signal, urges for further research of endospores as possible bioindicators for hydrocarbon seeps. If so, they could be a useful tool to constrain the different sources of methane escaping the shelf sediments of the ESAS.

5.4. Problems and uncertainties associated with cultivation and subsequent enumeration of endospores

To obtain an accurate estimate of the number of endospores of tSRB, a correct cultivation technique and a suitable choice of cultivation media must be chosen (which is not a fundamental task, as was discussed in section 5.2). The highest amount of accumulated sulfate reduced was only a modest ~3 mM in TGE #1 (incubated 96 h at brackish conditions, 8 mM sulfate, and with *Spirulina* as organic substrate), which is comparable to results obtained by de Rezende et al. (2013). They found a total amount of sulfate reduced of ca 2.6 mM after 120 h of incubation in sediment mixed with saltwater media (sulfate concentration 20 mM) and no addition of organic substrates. However, in slurries amended with a mixture of VFAs, around 5.5 mM were reduced. This led to the conclusion that the germinated endospores from TGE #1 were substrate limited, that the brackish water medium was not well-suited for the developed tSRBs, and/or that they needed a longer incubation time. Despite several studies indicating that VFAs are released upon incubation at high temperatures (Arnosti et al., 2004; Hubert et al., 2010; Graue et al., 2012; Volpi et al., 2017) it seems that sediments that have been pasteurized release less VFAs compared to unpasteurized sediments (Hubert et al., 2009; 2010), and it was therefore possible that the added *Spirulina* had not been enough as an organic source.

Hence, TGE #2 was designed using saltwater media with a sulfate concentration adjusted to 20 mM. *Spirulina* was complemented by acetate and pyruvate, and the incubation time was extended from 96 h up to 168 h. The resulting mesophilic signal stands out from the thermophilic signal from TGE #1, but the total amount of sulfate reduced was still not higher than 3 mM. Since the results from TGE #1 and #2 were perceived as a bit noisy, together with the modest drawdown of sulfate, contamination with oxygen was suspected. Contamination with oxygen would result in a re-oxidation of sulfide back to sulfate, thus obscuring the resulting signal interpreted from decreasing sulfate concentrations. TGE #3 was subsequently conducted using vials of the Hungate-type, which are designed for anaerobic cultivations. Moreover, a reducing agent in the form of Na_2S was added to persevere reducing conditions. Spirulina and acetate were complemented with propionate, butyrate, lactate and formate and the overall concentrations were increased. However, the maximum drawdown of sulfate (~1.5 mM) was even lower than in previous experiments, and an increasing trend in sulfate concentration strongly suggested vapour leakage as well as a potential oxygen contamination. Oxygen contamination would not only tangle with the results, but it would also diminish the reducing conditions that are required for successful cultivation of anaerobes. Before proceeding with a new experiment, a set of control experiments were designed.

The results from the control experiments confirmed that the Hungate tubes indeed lost weight during incubations, and more so with increasing temperatures. There was no strong correlation between the sulfate and sulfide concentrations, but an increasing trend in sulfate concentration from samples incubated in Hungate tubes could clearly be observed. This increase was not seen in corresponding sulfide concentrations. However, a decrease in sulfide would have been concealed by a concurrent increase in concentration due to loss of water. Another possibility explaining the lack of the anticipated sulfide increase is that volatile sulfide was lost together with water vapour, and/or by some other mechanism. Loss of sulfide has been shown to be strongly related to which type of rubber the stoppers are composed of. In a study by Elsgaard (2000), it was found that sulphidic samples closed with black rubber lost >3 times more sulfide compared to samples closed with butyl rubber. The mechanisms behind sulfide removal were not investigated, but it was thought that diffusion, absorption and/or adsorption to the stopper material were responsible (Elsgaard, 2000). Another possibility is that the screw caps were insufficient when an increased pressure started to build up due to sulfide production and increasing temperatures.

It has been reported that adding Na_2S as a reducing agent may be inhibitory for certain *Desulfotomaculum* sp. (Widdel&Bak, 1992). Hence, the effect of amending this reducing agent, as well as the effect of adding different organic substrates, were also tested. The results show that complementing *Spirulina* with a mixture of different VFAs clearly increases the accumulated amount of reduced sulfate. It is equally obvious that the addition of a reducing agent is beneficial for growth, as the sulfate consumption increases even more. This further strengthens the theory that the noisy results, as well as the diminished response in TGE #3, indeed depend on oxygen contamination. However, upon repeating the experiment in TGE #4, using the best suited vials (exetainers), additional VFAs, as well as a reducing agent, sulfate reduction was still completely absent. The reason for this can only be speculated upon, but is thought to depend on that germination was induced before pasteurization.

Once endospores have germinated, they become sensitive to sub-lethal heat treatments due to the release of Ca-DPA (among other things). This leads to an increase in water content and subsequently a decreased heat resistance (Nicholson et al., 2000; 2002; Setlow, 2007; Christie&Setlow, 2020). Endospores germinating "too early" was therefore likely killed during the ensuing pasteurization.

Germination could have been induced during handling of the original sediment stock at room temperature when initiating each experiment. Thus, due to a repeated handling of the sediment stock, relatively more endospores would have germinated when initiating TGE #4 compared to TGE #1, which may explain the absence of viable cells after pasteurization of sediment slurries in TGE #4. Another explanation may be that germination occurred during sample preparation. It was shown in a study by te Giffel et al. (1995) on *Bacillus cereus* (a thermoresistant, aerobic spore-forming bacteria found in food) that prolonged time between sample preparations and pasteurization would profoundly lead to an underestimation of initial endospore numbers. The number of germinated spores were also highly dependent on medium used. Within 30 minutes in room temperature 92% germination occurred, whereas ‘‘only’’ 23% germination occurred when using a saline solution. Germination decreased if the preparation was done at a temperature of 0℃, but up to 48% germination still occurred if preparations were performed using a media of pasteurized milk (te Giffel et al., 1995). These findings imply that more endospores might have germinated during the preparation of TGE #3 and #4, when sediment was amended with additional VFAs at higher concentrations compared to TGE #1 and #2, when only *Spirulina* and low concentrations of acetate and pyruvate were used. Moreover, the experiments included large numbers of samples, and the preparation time could at times amount to > 2 hours. Even if already prepared samples were stored refrigerated until pasteurization, the findings of te Giffel and colleagues demonstrate that large numbers of endospores may still have germinated during that time.

Further considerations when it comes to sample preparation is that the temperature and duration used for heat-activation/pasteurization seems to be chosen rather arbitrary. This is reflected by the variation for pasteurization procedures between studies. For example, for sample volumes between 6 to 11 ml, the temperature and duration for pasteurization range from 80℃ for 10 to 20 minutes (Widdel, 2006) to 80℃ for 60 minutes (Hubert et al., 2009). Only in one study was the temperature inside the vials during pasteurization actually monitored, which showed that the time needed to reach 80℃ in a 6 ml sample was approximately 10 minutes (Volpi et al., 2017). Why the temperature is set to 80℃ is not very clear.

The effect of a prolonged preparation time, the choice of cultivation media, and the temperature and time chosen for the heat pre-treatment, is only speculative without a thorough investigation targeting endospores from tSRB, but is likely to be significant. It is obvious from the results presented in this work however, that the physiological diversity together with the overall problems using cultivation-dependent methods lead to an *underestimation* of the true numbers of in situ endospores. In conclusion, it may be wise to test the stopper material for potential gaseous loss (i.e. water and sulfide), since loss of sulfide may impede the growth of anaerobic bacteria due to abating reducing conditions (Elsgaard, 2000). Furthermore, an enhanced loss of water may change concentrations and may confound the obtained results which may lead to underestimations of growth yields and/or erroneously interpretations. It may also be beneficial to use culturing vials closed with crimp seals instead of screw caps when conducting experiments with an expected pressure increase. It is also a good idea to keep the preparation time as short as possible, preferentially < 30 minutes or even shorter. Moreover, it could also be beneficial to pasteurize the sediment prior to mixing with the cultivation medium, or at least before amending with organic substrates. Preparations at as low temperatures as possible may also be considered.

One may also consider that it could be a good idea to use ‘‘standard media’’ when cultivating endospores from tSRB, such that it would be more comparable across investigations by employing equivalent conditions. However, as long as sediments are used as inocula, conditions will never be

equal from one location to another. For example, endospore abundances show high lithology-dependent variations, with higher numbers found in fine-grained, muddy sediments compared to sandy sediments (Fichtel et al., 2008). Furthermore, not all bacteria are able to grow under laboratory conditions (Staley&Konopka, 1985), which was also concluded by Turnbull et al. (2007), who found that obtained endospore numbers using ‘‘viable plate counts’’ differed significantly from counts determined microscopically. This indicated that not all endospores in a population were stimulated to germinate, or that they might have been non-viable (Turnbull et al., 2007). Thus, as long as we are using cultivation-dependent methods, there will always be some uncertainties associated with the obtained results, which are important to realize when doing cross-comparisons with results from other investigations, particularly if other cultivation conditions and/or other locations have been used.

Conclusion and Future Prospects

There is an undisputable presence of endospores of tSRB in the cold Baltic and Siberian shelf sediments. However, taxonomic identification could not be deduced within the scope of this project, and since it was not possible to infer their source environment based on salinity and temperature characteristics alone, their source habitat and dispersal history is still enigmatic. Based on these results, it is not possible to use them as oceanographic tracers at present. However, their ability to endure harsh conditions and withstand the test of time render them an undeniable potential to be used as tracer organisms. Another potential use, which have not been explored in this project but deserves future exploration, may be to screen for possible pollution.

Their possibility to be used in such multiple important research areas really advocates for further investigation concerning endospores of tSRB as tracer organisms. Questions that should be addressed such that their cultivation and subsequent identification and numeration can be made with higher certainties include how different cultivation techniques (choice of media, preparation-time, heat pre-treatment etc.) affect germination and growth (and subsequent enumeration and identification). Another issue not concerning cultivation, but which likely have a large effect on the endospore abundance, is related to sedimentation processes. Exactly how endospores are transported (i.e. as ‘‘free-floating’’ cells, aggregated to other particles etc.) within the water column have got little attention, and is also a subject that should be investigated since the interpretation of the spatial distribution of endospores depends on a good knowledge about local sedimentation factors as well as local hydrogeographic patterns.

Acknowledgments

First and foremost, I want to thank my supervisor Volker Brüchert for offering me this project. These misplaced microorganisms caught my interest from our first discussion, and they have intrigued me ever since. I am thankful for all the help during this project, but even more so for your insight that sometimes it is easier to work without a ‘‘watchful eye’’. Secondly, I want to thank all the people around me that have helped me with both small and big things. Julia for all the help in the lab, Sebastian for learning me how to perform distillations, Jonas and Thea for listening to my frustration when my experiments have gone bad, Pär for all the help with the sulfate analyses (they have been many!), and Susanne for all the encouragement and input on my work, you are an angel! Lastly, I want to thank my ever-supporting family, for providing me with love and lots of coffee!

References

Agogué H., Lamy, D., Neal, P.R., Sogin, M.L., Herndl, G.J. (2011). Water mass-specificity of bacterial communities in the North Atlantic revealed by massively parallel sequencing. *Molecular Ecology*. 20, p258–274.

Anandkumar, B., Choi, J.-H., Venkatachari, G., Maruthamuthu, S. (2009). Molecular characterization and corrosion behavior ofthermophilic (55 8C) SRB Desulfotomaculum kuznetsoviiisolated from cooling tower in petroleum refinery. *Materials and Corrosion*. 60 (9), p730-737.

Anderson, L.G., Björk, G., Holby, O., Jutterström, S., Mörth, C.-M., O'Regan, M., Pearce, P., Semiletov, I., Stranne, C., Stöven, T., Tanhua, T., Ulfsbo, A., Jakobsson, M. (2017). Shelf–Basin interaction along the East Siberian Sea. *Ocean Science*. 13, p349-363.

Arnosti, C., Finke, N., Larsen, O., Ghobrial, S. (2004). Anoxic carbon degradation in Arctic sediments: Microbial transformations of complex substrates. *Geochimica et Cosmochimica Acta*. 69 (9), p2309-2320.

Aüllo, T., Ranchou-Peyruse, A., Ollivier, B., Magot, M. (2013). Desulfotomaculum spp. and related gram-positive sulfate-reducing bacteria in deep subsurface environments. *Frontiers in Microbiology*. 4 (362), p1-12.

Bak, F., Scheff, G., Jansen, K.-H. (1991). A rapid and sensitive ion chromatographic technique for the determination of sulfate and sulfate reduction rates in freshwater lake sediments. *Federation of European Microbiological Societies*. 85, p23-30.

Barnes, S.P., Bradbrook, S.D., Cragg, B.A., Marchesi, J.R., Weightman, A.J., Fry, J.C., Parkes, R.J. (1998). Isolation of sulfate-reducing bacteria from deep sediment layers of the pacific ocean. *Geomicrobiology Journal*. 15 (2), p67-83.

Baranov, B., Galkin, S., Vedenin, A., Dozorova, K., Gebruk, A., Flint, M. (2020). Methane seeps on the outer shelf of the Laptev Sea: characteristic features, structural control, and benthic fauna. *Geo-Marine Letters*. 40, p541–557.

Basso, O., Lascourreges, J.-F., Le Borgne. F., Le Goff, C., Magot, M. (2009). Characterization by culture and molecular analysis of the microbial diversity of a deep subsurface gas storage aquifer. *Research in Microbiology*. 160, p107-116.

Bauch, H.A., Kassens, H., Naidina, O.D., Kunz-Pirrung, M., Thiede, J. (2001). Composition and Flux of Holocene Sediments on the Eastern Laptev Sea Shelf, Arctic Siberia. *Quarternary Research*. 55, p344-351.

Bell, S. (2001). Good Practice Guide No. 11 The Beginner's Guide to Uncertainty of Measurement. *National Physical Laboratory*. p1-34.

Bell, E., Blake, L.I., Sherry, A., Head, I.H., Hubert, C.R.J. (2018). Distribution of thermophilic endospores in a temperate estuary indicate that dispersal history structures sediment microbial communities. *Environmental Microbiology*. 20 (3), p1134–1147.

Bell, E., Sherry, A., Pilloni, G., Suárez-Suárez,A., Cramm, M.A., Cueto, G., Head, I.M., Hubert, C.R.J. (2020). Sediment cooling triggers germination and sulfate reduction by heat-resistant thermophilic spore-forming bacteria. *Environmental Microbiology*. 22 (1), p456-465.

Campbell, L.L. & Postgate, J.R. (1965). Classification of the Spore-Forming Sulfate-Reducing Bacteria. *Bacteriological Reviews*. 29 (362), p359-363.

Cano, R.J. & Borucki, M.K. (1995). Revival and Identification of Bacterial Spores in 25- to 40-Million-Year-Old Dominican Amber. *Science*. 268 (5213), p1060-1064.

Castro, H.F., Williams, N.H., Ogram, A. (2000). Phylogeny of sulfate-reducing bacteria. *Federation of European Microbiological Societies*. 31, p1-9.

Cha, I-T., Roh, S.W., Kim, S-J., Hong, H-J., Lee, H-W., Lim, W-T., Rhee, S-K. (2013). Desulfotomaculum tongense sp. nov., a moderately thermophilic sulfate-reducing bacterium isolated from a hydrothermal vent sediment collected from the Tofua Arc in the Tonga Trench. *Antonie van Leeuwenhoek*. 104, p1185–1192.

Chivian, D., Brodie, E.L., Alm, E.J., Culley, D.E., Dehal, P.S., DeSantis, T.Z., Gihring, T.M., Lapidus, A., Lin, L-H., Lowry, S.R., Moser, D.P, Richardson, P.M., Southam, Wanger, G., Pratt, L.M., And. (2008). Environmental Genomics Reveals a Single-Species Ecosystem Deep Within Earth. *Science*. 322 (5899), p275-278.

Christie, G. & Setlow, P. (2020). Bacillus spore germination: Knowns, unknowns and what we need to learn. *Cellular Signalling*. 74, p1-9.

Cline, J.D. (1969). Spectrophotometric Determination of Hydrogen Sulfide in Natural Waters. *Limnology and Oceanography*. 14 (3), p454-458.

Cowan, A.E., Koppel, D.E., Setlow, B., Setlow, P. (2003). A soluble protein is immobile in dormant spores of Bacillus subtilis but is mobile in germinated spores: Implications for spore dormancy. *Proceedings of the National Academy of Sciences of the United States of America*. 100 (7), p4209–4214.

Cramer, B. & Franke, D. (2005). Indications For an Active Petroleum System in the Laptev Sea, NE Siberia. *Journal of Petroleum Geology*. 28 (4), p369-384.

Cypionka, H. & Pfennig, N. (1986). Growth yields of Desulfotomaculum orientis with hydrogen in chemostat culture. *Archives of Microbiology*. 143, p396-399.

Davidson, M.M., Bisher, M.E., Pratt, L.M., Fong, J., Southam, G., Pfiffner, S.M., Reches, Z., Onstott, T.C. (2009). Sulfur Isotope Enrichment during Maintenance Metabolism in the Thermophilic Sulfate-Reducing Bacterium Desulfotomaculum putei. *Applied and Environmental Microbiology*. 75 (17), p5621-5630.

de Rezende, J.R., Hubert, C.R.J., Røy, H., Kjeldsen, K.U., Jørgensen, B.B. (2017). Estimating the Abundance of Endospores of Sulfate-Reducing Bacteria in Environmental Samples by Inducing Germination and Exponential Growth. *Geomicrobiology Journal*. 34 (4), p338-345.

de Rezende, J.R., Kjeldsen, K.U., Hubert, C.R.J., Finster, K., Loy, A., Jørgensen, B.B. (2013). Dispersal of thermophilic Desulfotomaculum endospores into Baltic Sea sediments over thousands of years. *International Society for Microbial Ecology*. 77, p72-84.

Detmers, J., Brüchert, V., Habicht, K.S., Kuever, J. (2001). Diversity of Sulfur Isotope Fractionations by Sulfate-Reducing Prokaryotes. *Applied and Environmental Microbiology*. 67 (2), p888–894.

Donnelly, L.S. & Busta, F.F. (1982). Characterization of Germination of Desulfotomaculum nigrificans Spores. *Journal of Food Protection*. 45 (8), p721-728.

Edmonds, H.N., Michael, P.J., Baker, E.T., Connelly, D.P., Snow, J.E., Langmuir, C.H., Dick, H.J.B., Muhe, R., German, C.R., Graham, D.W. (2003). Discovery of abundant hydrothermal venting on the ultraslow-spreading Gakkel ridge in the Arctic Ocean. *Nature*. 421, p252-256.

Elsgaard, L. (2000). Rubber stoppers used with sulphidic media: a note of caution. *World Journal of Microbiology & Biotechnology*. 16, p571-572.

Evans, F. & Curran, H.R. (1943). The Accelerating Effect of Sublethal Heat On Spore Germination In Mesophilic Aerobic Bacteria. *Journal of Bacteriology*. 46 (6), p513-523.

Fichtel, J., Köster, J., Rullkötter, J., Sass, H. (2008). High Variations in Endospore Numbers within Tidal Flat Sediments Revealed by Quantification of Dipicolinic Acid. *Geomicrobiology Journal*. 25, p371–380.

Fossing, H. (1995). 35S-Radiolabeling To Prope Biogeochemical Cycling of Sulfur. In: Vairavamurthy, M.A., Schoonen, M.A.A., Eglinton, T.I., Luther, G.W., Manowitz, B *Geochemical Transformations of Sedimentary Sulfur*. American Chemical Society Symposium Series. 612, p348-364.

Foster, S.J. & Johnstone, K. (1990). Pulling the trigger: the mechanism of bacterial spore germination. *Molecular Microbiology*. 4 (1), p137-141.

Frank, Y., Banks, D., Avakian, M., Antsiferov, D., Kadychagov, P., Karnachuk, O. (2016). Firmicutes is an Important Component of Microbial Communities in Water-Injected and Pristine Oil Reservoirs, Western Siberia, Russia. *Geomicrobiology Journal*. 33 (5), p387–400.

Garrity, G.M. (2016). A New Genomics-Driven Taxonomy of Bacteria and Archaea: Are We There Yet?. *Journal of Clinical Microbiology*. 54 (8), p1956–1963.

Gerasimchuk, A.L., Shatalov, A.A., Novikov, A.L., Butorova, O.P., Pimenov, N.V., Lein, A.Y., Yanenko, A.S., Karnachuk, O.V. (2010). The Search for SulfateReducing Bacteria in Mat Samples from the Lost City Hydrothermal Field by Molecular Cloning. *Microbiology*. 79 (1), p96–105.

te Giffel, M.C., Beumer, R.R., Hoekstra, J., Rombouts, F.M. (1995). Germination of bacterial spores during sample preparation. *Food Microbiology*. 12, p327-332.

Goorissen, H.P., Boschker, H.T.S., Stams, A.J.M., Hansen, T.A. (2003). Isolation of thermophilic Desulfotomaculum strains with methanol and sulfite from solfataric mud pools, and characterization of Desulfotomaculum solfataricum sp. nov.. *International Journal of Systematic and Evolutionary Microbiology*. 53, p1223-1229.

Graue, J., Engelen, B., Cypionka, H. (2012). Degradation of cyanobacterial biomass in anoxic tidal-flat sediments: a microcosm study of metabolic processes and community changes. *International Society for Microbial Ecology*. 6, p660-669.

Guan, J., Xia, L-P., Wang, L-Y., Liu, J-F., Gu, J-D., Mu, B-Z. (2013). Diversity and distribution of sulfate-reducing bacteria in four petroleum reservoirs detected by using 16S rRNA and dsrAB genes. *International Biodeterioration & Biodegradation*. 76, p58-66.

Hagen, S.J. (2010). Exponential growth of bacteria: Constant multiplication through division. *American Journal of Physics*. 78, p1290-1296.

Hansen, T.A. (1994). Metabolism of sulfate-reducing prokaryotes. *Antonie van Leeuwenhoek*. 66, p165-185.

Hanson, C.A., Fuhrman, J.A., Horner-Devine, M.C., Martiny, J.B.H. (2012). Beyond biogeographic patterns: processes shaping the microbial landscape. *Nature Reviews Microbiology*. 10, p497-506.

Hanson, C.A., Müller, A.L., Loy, A., Dona, C., Appel, R., Jørgensen, B.B., Hubert, C.R.J. (2019). Historical Factors Associated With Past Environments Influence the Biogeography of Thermophilic Endospores in Arctic Marine Sediments. *Frontiers in Microbiology*. 10 (245), p1-14.

Hubert, C. & Judd, A. (2010). 23 Using Microorganisms as Prospecting Agents in Oil and Gas Exploration. In: Timmis, K.N. *Handbook of Hydrocarbon and Lipid Microbiology*. Berlin, Heidelberg: Springer. p2713-2725.

Hubert, C., Loy, A., Nickel, M., Arnosti, C., Baranyi, C., Brüchert, V., Ferdelman, T., Finster, K., Christensen, F.M., de Rezende, J.R., Vandieken, V., Jørgensen, B.B. (2009). A Constant Flux of Diverse Thermophilic Bacteria into the Cold Arctic Seabed. *Science*. 325 (5947), p1541-1544.

Isaksen, M.F., Bak, F., Jørgensen, B.B. (1994). Thermophilic sulfate-reducing bacteria in cold marine sediment. *Federation of European Microbiological Societies*. 14, p1-8.

Kaksonen, A.H., Spring, S., Schumann, P., Kroppenstedt, R.M., Puhakka, J.A. (2007a). Desulfovirgula thermocuniculi gen. nov., sp. nov., a thermophilic sulfate-reducer isolated from a geothermal underground mine in Japan. *International Journal of Systematic and Evolutionary Microbiology*. 57 (a), p98-102.

Kaksonen, A.H., Spring, S., Schumann, P., Kroppenstedt2, R.M., Puhakka, J.A. (2007b). Desulfurispora thermophila gen. nov., sp. nov., a thermophilic, spore-forming sulfate-reducer isolated from a sulfidogenic fluidized-bed reactor. *International Journal of Systematic and Evolutionary Microbiology*. 57, p1089–1094.

Kallmeyer, K., Ferdelman, T.G., Weber, A., Fossing, H., Jørgensen, B.B. (2004). A cold chromium distillation procedure for radiolabeled sulfide applied to sulfate reduction measurements. *Limnology and Oceanography: Methods*. 2, p171-180.

Karnachuk, O.V., Frank, Y.A., Lukina, A.P., Kadnikov, V.V., Beletsky, A.V., Mardanov, A.V., Ravin, N.V. (2019). Domestication of previously uncultivated Candidatus Desulforudis audaxviator from a deep aquifer in Siberia sheds light on its physiology and evolution. *International Society for Microbial Ecology*. 13, p1947–1959.

Korneeva, V.A., Pimenov, N.V., Krek, A.V., Tourova, T.P., Bryukhanov, A.L. (2015). Sulfate-Reducing Bacterial Communities in the Water Column of the Gdansk Deep (Baltic Sea). *Microbiology*. 84 (2), p268-277.

Larsson, U., Elmgren, R., Wulff, F. (1985). Eutrophication and the Baltic Sea: Causes and Consequences. *Ambio*. 14 (1), p9-14.

Leppäranta, M. & Myrberg, K (2009). *Physical Oceanography of the Baltic Sea*. Berlin: Springer Science+Business Media. p378.

Lowell, R.P., Kolandaivelu, K., Rona, P.A. (2014). Hydrothermal Activity. *Reference Module in Earth Systems and Environmental Sciences*. p1-19.

Magot, M., Ollivier, B., Patel, B.K.C. (2000). Antonie van Leeuwenhoek Journal of Microbiology. *Microbiology of petroleum reservoirs*. 77, p103-116.

Maier, R.M. & Pepper, I.L. (2015). Bacterial Growth. In: Pepper, I.L., Gerba, C.P., Gentry *Environmental Microbiology*. 3rd ed. Elsevier. p37-56.

Marietou, A., Røy, H., Jørgensen, B.B., Kjeldsen, K.U. (2018). Sulfate Transporters in Dissimilatory Sulfate Reducing Microorganisms: A Comparative Genomics Analysis. *Frontiers in Microbiology*. 9 (309), p1-21.

Martiny, J.B.H., Bohannan, B.J.M., Brown, J.H., Colwell, R.K., Fuhrman, J.A., Green, J.L., Horner-Devine, M.C., Matthew Kane, M., Krumins, J.A., Kuske, C.R., Morin, P.J., Naeem, S., Øvreås, L., Reysenbach, A.-L., Smith, V.H., Staley, J.T. (2006). Microbial biogeography: putting microorganisms on the map. *Nature Reviews Microbiology*. 4, p102-112.

Meier, H.E.M. & Kauker, F. (2003). Sensitivity of the Baltic Sea salinity to the freshwater supply. *Climate Research*. 24, p231-242.

Muyzer, M. & Stams, A.J.M. (2008). The ecology and biotechnology of sulphate-reducing bacteria. *Nature Reviews Microbiology*. 6, p441-454.

Müller, A.L., de Rezende, J.R., Hubert, C.R.J., Kjeldsen, K.U., Lagkouvardos, I., Berry, D., Jørgensen, B.B., Loy, A. (2014). Endospores of thermophilic bacteria as tracers of microbial dispersal by ocean currents. *International Society for Microbial Ecology*. 8, p1153-1165.

Müller, A.L., Pelikan, C., de Rezende, J.R., Wasmund, K., Putz, M., Glombitza, C., Kjeldsen, K.U., Jørgensen, B.B., Loy, A. (2018). Bacterial interactions during sequential degradation of cyanobacterial necromass in a sulfidic arctic marine sediment. *Environmental Microbiology*. 20 (8), p2927-2940.

Nicholson, W.L., Fajardo-Cavazos, P., Rebeil, R., Slieman, T.A., Riesenman, P.J., Law, J.F., Xue, Y. (2002). Bacterial endospores and their significance in stress resistance. *Antonie van Leeuwenhoek*. 81, p27–32.

Nicholson, W.L., Munakata, N., Horneck, G., Melosh, H.J., Setlow, P. (2000). Resistance of Bacillus Endospores to Extreme Terrestrial and Extraterrestrial Environments. *Microbiology and Molecular Biology Reviews*. 64 (3), p548-572.

Paidhungat, M. & Setlow, P. (2002). Spore Germination and Outgrowth. In: Sonenshein, A.L., Hoch, J.A., Losick, R *Bacillus subtilis and Its Closest Relatives: From Genes to Cells*. Washington: American Society for Microbiology. p537-548.

Paredes-Sabja, D., Setlow, P., Sarker, M.R. (2011). Germination of spores of Bacillales and Clostridiales species: mechanisms and proteins involved. *Trends in Microbiology*. 19 (2), p85-94.

Parkes, R.J. & Sass, H. (2009). The sub-seafloor biosphere and sulphate-reducing prokaryotes: their presence and significance. In: Barton L.L. & Hamilton, W.A *Sulphate-reducing Bacteria Environmental and Engineered Systems*. Cambridge: Cambridge University Press. p329-358.

Parshina, S.N., Sipma, J., Nakashimada, Y., Henstra, A.M., Smidt, H., Lysenko, A.M., Lens, P.N.L., Lettinga, G., Stams, A.J.M. (2005). Desulfotomaculum carboxydivorans sp. nov., a novel sulfate-reducing bacterium capable of growth at 100% CO. *International Journal of Systematic and Evolutionary Microbiology*. 55, p2159–2165.

Pepper, I.L. & Gerba, C.P. (2015). Cultural Methods. In: Pepper, I.L., Gerba, C.P., Gentry, T.J *Environmental Microbiology*. 3rd ed. Elsevier. p195-212.

Rabus, R., Venceslau, S.S., Wöhlbrand, L., Voordouw, G., Wall, J.D., Pereira, I.A.C. (2015). A Post-Genomic View of the Ecophysiology, Catabolism and Biotechnological Relevance of Sulphate-Reducing Prokaryotes. *Advances in Microbial Physiology*. 66, p55-321.

Rosnes, J.T., Torsvik, T., Lien, T. (1991). Spore-Forming Thermophilic Sulfate-Reducing Bacteria Isolated from North Sea Oil Field Waters. *Applied and Environmental Microbiology*. 57 (8), p2302-2307.

Røy, H., Weber, H.S., Tarpgaard, I.H., Ferdelman, T.G., Jørgensen, B.B. (2014). Determination of dissimilatory sulfate reduction rates in marine sediment via radioactive 35S tracer. *Limnology and Oceanography: Methods*. 12, p196-211.

Sapart, C., Shakhova, N., Semiletov, I., Jansen, J., Szidat, S., Kosmach, D., Dudarev, O., van der Veen, C., Egger, M., Sergienko, V., Salyuk, A., Tumskoy, V., Tison, J-L., Röckmann, T. (2017). The origin of methane in the East Siberian Arctic Shelf unraveled with triple isotope analysis. *Biogeosciences*. 14, p2283–2292.

Sass, H., Overmann, J., Rütters, H., Babenzien, H-D., Cypionka, H. (2004). Desulfosporomusa polytropa gen. nov., sp. nov., a novel sulfate-reducing bacterium from sediments of an oligotrophic lake. *Archives of Microbiology*. 182, p204–211.

Setlow, P. (2006). Spores of Bacillus subtilis: their resistance to and killing by radiation, heat and chemicals. *Journal of Applied Microbiology*. 101, p514–525.

Setlow, P. (2007). I will survive: DNA protection in bacterial spores. *Trends in Microbiology*. 15 (4), p172-180.

Setlow, P., Wang, S., Li, Y.-Q. (2017). Germination of Spores of the Orders Bacillales and Clostridiales. *Annual Reviews Microbiology*. 71, p459-477.

Stackebrandt, E., Sproer, C., Rainey, F.A., Burghardt, J., Pauker, O., Hippe, H. (1997). Phylogenetic Analysis of the Genus Desulfotomaculum: Evidence for the Misclassification of Desulfotomaculum guttoideum and Description of Desulfotomaculum orientis as Desulfosporosinus orientis gen. n. *International Journal of Systematic Bacteriology*. 47 (4), p1134-1139.

Staley, J.T. & Konopka, A. (1985). Measurement of In Situ Activities of Nonphotosynthetic Microorganisms in Aquatic and Terrestrial Habitats. *Annual Reviews Microbiology*. 39, p321-346.

Steinbach, J., Holmstrand, H., Shcherbakovad, K., Kosmachd, D., Brüchert, V., Shakhovae, N., Salyukd, N., Saparth, C.J., Chernykhd, D., Noormets, R., Semiletov, I., Gustafsson, Ö. (2021). Source apportionment of methane escaping the subsea permafrost system in the outer Eurasian Arctic Shelf. *Proceedings of the National Academy of Sciences of the United States of America*. 118 (10), p1-9.

Stubner, S. & Meuser, K. (2000). Detection of Desulfotomaculum in an Italian rice paddy soil by 16S ribosomal nucleic acid analyses. *0 Federation of European Microbiological Societies*. 34, p73-80.

SWERUS Scientific Party. (2016). The Swedish-Russian-US Arctic Ocean Investigation of Climate-Cryosphere-Carbon Interactions Cruise Report – Leg 1 (of 2). *Meddelanden från Stockholms Universitets Bolin Centre for Climate Research*. 1, p1-200.

Tan, I.S. & Ramamurthi, K.S. (2014). Spore formation in Bacillus subtilis. *Environmental Microbiology Reports*. 6 (3), p212-225.

Vatsurina, A., Badrutdinova, D., Schumann, P., Spring, S., Vainshtein, M. (2008). Desulfosporosinus hippei sp. nov., a mesophilic sulfate-reducing bacterium isolated from permafrost. *International Journal of Systematic and Evolutionary Microbiology*. 58, p1228–1232.

Vecchia, E.D., Visser, M., Stams, A.J.M., Bernier-Latmani, R. (2014). Investigation of sporulation in the Desulfotomaculum genus: a genomic comparison with the genera Bacillus and Clostridium. *Environmental Microbiology Reports*. 6 (6), p756-766.

Volpi, M., Lomstein, B.A., Sichert, A., Røy, H., Jørgensen, B.B., Kjeldsen, K.U. (2017). Identity, Abundance, and Reactivation Kinetics of Thermophilic Fermentative Endospores in Cold Marine Sediment and Seawater. *Frontiers in Microbiology*. 8, p1-13.

Widdel, F. (2006). The Genus Desulfotomaculum. In: Dworkin, M., Falkow, S., Rosenberg, E., Schleifer, K.H., Stackebrandt, E *Prokaryotes Volume 4*. 3rd ed. New York: Springer Science+Business Media. p787-794.

Widdel, F. & Bak, F. (1992). Gram-Negative Mesophilic Sulfate-Reducing Bacteria. In: Balows, A., Truper, H.G., Dworkin, M., Harder, W., Schleifer, K-H. *The Prokaryotes*. 2nd ed. New York: Springer Science+Business Media. p3352-3378.

Wunderlin, T., Junier, T., Roussel-Delif, L., Jeanneret, N., Junier, P. (2013). Stage 0 sporulation gene A as a molecular marker to study diversity of endospore-forming Firmicutes. *Environmental Microbiology Reports*. 5 (6), p911–924.

Wörmer, L., Hoshino, T., Bowles, M.W., Viehweger, B., Adhikari, R.R., Xiao, N., Uramoto, G., Könneke, M., Lazar, C.S., Morono, Y., Inagaki, F., Hinrichs, K-U. (2019). Microbial dormancy in the marine subsurface: Global endospore abundance and response to burial. *Science Advances*. 5 (2), p1-8.

Zhang, P., Garner, W., Yi, X., Yu, J., Li, Y-q., Setlow, P. (2010). Factors Affecting Variability in Time between Addition of Nutrient Germinants and Rapid Dipicolinic Acid Release during Germination of Spores of Bacillus Species. *Journal of Bacteriology*. 192 (14), p3608–3619.

Appendices

Appendix A

Artificial seawater and Basal media

All media were mixed with mQ up to a total volume of 1 l and autoclaved by saturated steam sterilization at 121℃ for 30 min and stored refrigerated until use.

TGE #1

*Table 1: Artificial seawater medium prepared according to Widdel&Bak (1992), adjusted to brackish concentrations. *not included in original recipe.*

Substance	g	mM
NaCl	7.43	127.1
$MgSO_4x7H_2O$	1.94	7.9
$MgCl_2x6H_2O$	1.60	7.9
KCl	0.21	2.8
$CaCl_2x2H_2O$	0.40	2.7
NH_4Cl	0.25	4.7
KH_2PO_4	0.20	1.5
$NaHCO_3$*	0.20	2.4

TGE #2

*Table 2: Artificial seawater medium prepared according to Widdel&Bak (1992) with sulfate adjusted to 20 mM. *not included in original recipe.*

Substance	g	mM
NaCl	26.00	444.9
$MgSO_4x7H_2O$	4.93	20.0
$MgCl_2x6H_2O$	5.60	27.5
KCl	0.72	9.7
$CaCl_2x2H_2O$	1.40	9.5
NH_4Cl	0.25	4.7
KH_2PO_4	0.20	1.5
$NaHCO_3$*	0.20	2.4

TGE #3 and #4

*Table 3: Basal fresh-, brackish-, and saltwater media prepared according to Widdel&Bak (1992). *not included in original recipe.*

	Fresh		**Brackish**		**Salt**	
Substance	g	mM	g	mM	g	mM
NaCl	0.00	0.0	7.00	119.8	20.00	342.2
$MgCl_2x6H_2O$	0.40	2.0	1.20	5.9	3.00	14.8
$CaCl_2x2H_2O$	0.10	0.7	0.10	0.7	0.15	1.0
Na_2SO_4	4.00	28.2	4.00	28.2	4.00	28.2
NH_4Cl	0.25	4.7	0.25	4.7	0.25	4.7
KH_2PO_4	0.20	1.5	0.20	1.5	0.20	1.5
KCl	0.50	6.7	0.50	6.7	0.50	6.7
$NaHCO_3$*	0.20	2.4	0.20	2.4	0.20	2.4

Other amendments

Spirulina

Spirulina powder from Renée Voltaire was used in all experiments. The carbon and nitrogen content were analysed using a Carlo Erba NC2500 with a Thermo Fischer Scientific delta-V isotope ratio mass spectrometer. The average carbon content was 45.5% and the nitrogen content 10.4%.

Pyruvate solution (2.0 M)

22.0 g sodium pyruvate dissolved in 100 ml mQ. Filter sterilized and stored refrigerated in the dark.

Acetate solution (2.0 M)

27.2 g CH3COONa x 3H2O dissolved in 100 ml mQ. Autoclaved by saturated steam sterilization at 121℃ for 30 min and stored refrigerated until use.

Propionate solution (2.0 M)

19.2 g $C_3H_5NaO_2$ dissolved in 100 ml mQ. Autoclaved as described above and kept refrigerated until use.

Formate solution (2.0 M)

13.6 g HCOONa dissolved in mQ, autoclaved, and kept refrigerated.

Lactate solution (2.0 M)

22. 4 g $NaC_3H_5O_3$ dissolved in mQ, autoclaved, and kept refrigerated.

Butyrate solution (1.0 M)

9.2 ml Butyric acid was mixed with 40 ml mQ whereby 24 ml NaOH (4.0 M) was added slowly under stirring. The pH was adjusted to between 8 and 9 by dropwise addition of NaOH. Ester was removed by gentle boiling. mQ was added to a final volume of 100 ml and the solution was autoclaved and subsequently kept refrigerated.

Sulfide solution (0.2 M)

Large crystals of Na_2S x $9H_2O$ were thoroughly cleaned with mQ and dried so as to yield a final weight of 4.8 g, which was dissolved in mQ under a constant flow of N_2. The final solution was autoclaved and stored in the fridge under a headspace of N_2.

Appendix B

Preparation of cold chromium chloride-hydrochloric acid distillation

Citrate buffer for aerosol trap (0.1 M)

19.2 g citric acid was dissolved in 1000 ml mQ and 4 g NaOH. pH was adjusted to ca 4.

ZnAc for H_2S trap (5%)

50 g Zinc acetate was dissolved in mQ to a final volume of 1000 ml.

Reduction of chromium chloride-hydrochloric acid for liberation of H_2S (1.0 M in 2N HCl)

96 ml HCl (37%) was added slowly to 516 g mQ, after which 150 g chromium chloride hexahydrate was added. Ca 0.5 kg zinc pellets was covered with 2N HCl and purged ca 20 minutes with N_2 in a reaction flask, after which the HCl was removed and disposed while maintaining N_2-atmosphere. The chromium-hydrochloric acid solution was subsequently poured over the cleaned zinc pellets while continuously purging with N_2. The chromium was reduced when the colour had changed from a mossy green (Cr^{3+}) to a clear blue (Cr^{2+}) colour (Fig. 19 and 20). The solution was drawn into 60 ml syringes and kept refrigerated until use. All preparations were performed under the fume-hood and wearing protective goggles.

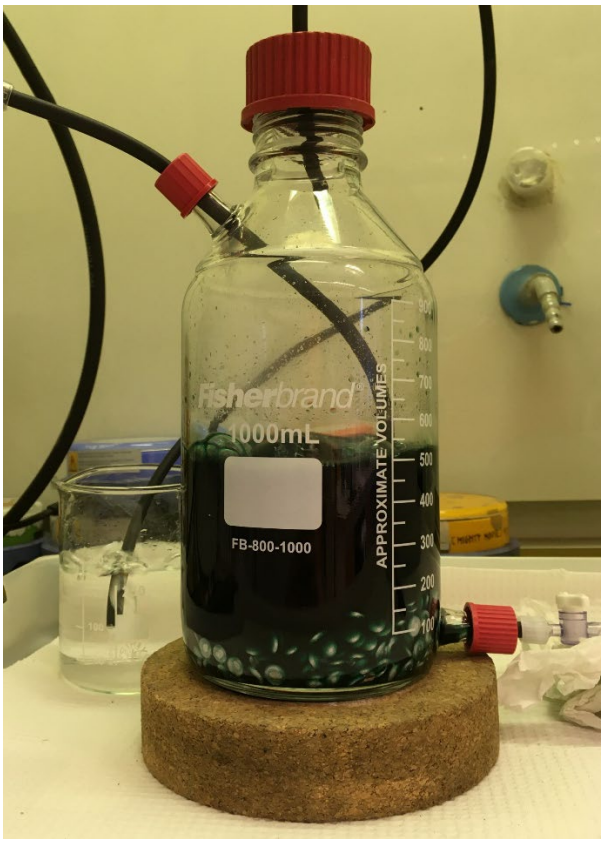

Figure 19: Mossy green oxidized chromium chloride.

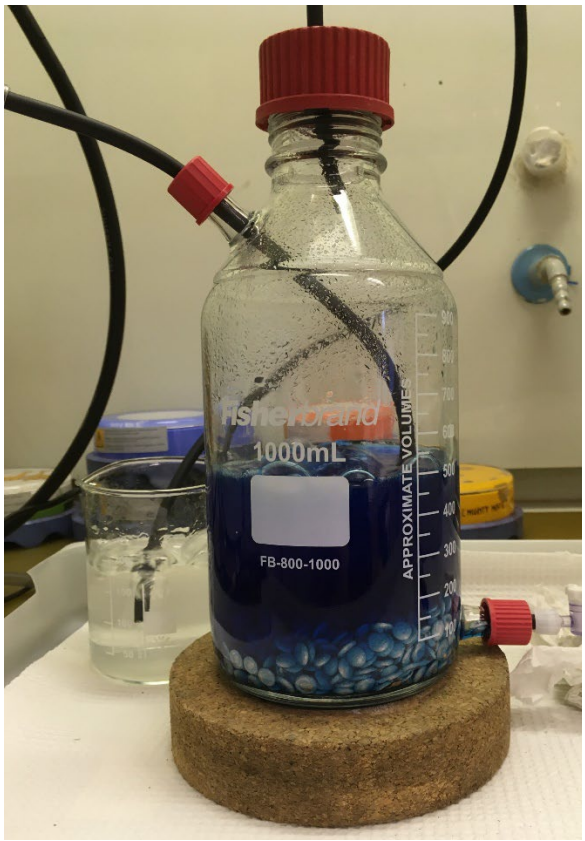

Figure: Clear blue reduced chromium chloride.

Appendix C

Uncertainty calculations

Replicate samples were used to calculate the expanded uncertainty using following set of equations:

The *estimated standard deviation* (*s*) was calculated by:

$$s = \sqrt{\frac{\sum_{i=1}^{n}(x_i - \bar{x})^2}{n-1}}$$

where x_i is the result of the *i*th measurement and $\bar{x}$ is the mean of the number of results (*n*). The *estimated standard uncertainty of the mean* (*u*), was then calculated by following formula:

$$u = \frac{s}{\sqrt{n}}$$

Finally, the *expanded standard uncertainty* (*U*) was multiplied with a coverage factor (*k* = 2) to provide a confidence level of approximately 95%.

$$U = 2u$$

The relative uncertainty (U_r) was reported for estimated SRRs, which had a large range in the obtained results. The relative uncertainty was calculated by:

$$U_r = \frac{U}{\bar{x}} \times 100$$

(Bell, 2001)